RESEARCH ARTICLE

The hypoxic response extends lifespan through a bioaminergic and peptidergic neural circuit

Elizabeth S Kitto[1†], Shijiao Huang[2†], Mira Bhandari[1], Cassie Tian[1], Rebecca L Cox[1], Safa Beydoun[1], Emily Wang[3], Danielle Shave[1], Hillary Miller[4], Sarah A Easow[1], Ella Henry[1], Eugene Chung[1], Megan L Schaller[1], Scott F Leiser[1,5]*

[1]Molecular and Integrative Physiology Department; University of Michigan, Ann Arbor, United States; [2]Department of Biochemistry and Molecular Biophysics, Kansas State University, Manhattan, United States; [3]Department of Cellular and Developmental Biology; University of Michigan, Ann Arbor, United States; [4]Cellular and Molecular Biology Program, University of Michigan, Ann Arbor, United States; [5]Department of Internal Medicine; University of Michigan, Ann Arbor, United States

eLife Assessment

This **fundamental** study, supported by **convincing** evidence, identifies the specific neuronal components that enable HIF-1 signaling in specific serotonergic neurons to regulate effectors in peripheral tissues. Specifically, stabilizing HIF-1 in ADF and NSM serotonergic neurons is sufficient to extend lifespan and healthspan in *C. elegans*, and these physiological benefits require several oxygen-sensing neurons, as well as neurotransmitters (GABA and tyramine), and a neuropeptide (NLP-17). The strengths of the study include rigorous experimental design, high quality data, the use of multiple genetic tools, and functional dissection using the well-validated *C. elegans* model.

***For correspondence:** leiser@med.umich.edu

[†]These authors contributed equally to this work

Competing interest: See page 18

Funding: See page 19

Preprint posted
09 May 2025
Sent for Review
27 May 2025
Reviewed preprint v1
26 August 2025
Reviewed preprint v2
17 September 2026
Version of Record
06 November 2026

Reviewing Editor: Sylvia Lee, Cornell University, United States

© Copyright Kitto, Huang *et al*. This article is distributed under the terms of the Creative Commons Attribution License, which permits unrestricted use and redistribution provided that the original author and source are credited.

Abstract A coordinated response to stress is crucial for promoting the short- and long-term health of an organism. The perception of stress, frequently through the nervous system, can lead to physiological changes that are fundamental to maintaining homeostasis. Activating the response to low oxygen, or hypoxia, extends healthspan and lifespan in *Caenorhabditis elegans*. However, despite some positive impacts, negative effects of the hypoxic response in specific tissues prevent translation of their benefits in mammals. Thus, it is imperative to identify which components of this response promote longevity. Here, we interrogate the cell-nonautonomous signaling pathway downstream of genetic activation of the hypoxic response. We find that HIF-1-mediated signaling in ADF serotonergic neurons is both necessary and sufficient for lifespan extension. Signaling through the serotonin receptor SER-7 in the GABAergic RIS interneurons is necessary in this process. Our findings also highlight the involvement of additional neural signaling molecules, including the neurotransmitters tyramine and GABA, and the neuropeptide NLP-17, in mediating longevity effects. Finally, we demonstrate that oxygen- and carbon-dioxide-sensing neurons act downstream of HIF-1 in this circuit. Together, these insights demonstrate a circuit for how genetic induction of the hypoxic response cell-nonautonomously modifies aging and suggests valuable targets for modulating aging in mammals.

Introduction

The global population is aging at an unprecedented rate, posing significant challenges for healthcare systems worldwide (**Burch et al., 2014**). The increasing burden of age-related diseases such as cardiovascular disease, diabetes, and neurodegeneration (**Kaeberlein, 2013**) highlights the pressing need to improve healthspan, defined as the disease-free period of life (**Kirkland and Peterson, 2009**). Work over the past several decades has led to a better understanding of the conserved molecular and cellular mechanisms that regulate lifespan. One promising avenue has been the identification of environmental stressors that, when applied in a controlled manner, activate stress-response pathways to promote longevity. These interventions, including calorie restriction, exercise, hypoxia, heat shock, and cold exposure, extend lifespan and healthspan (**Fontana and Partridge, 2015**; **Conti, 2008**; **Zhang et al., 2009**; **Stewart et al., 2013**). These stress-response pathways induce hormesis, a phenomenon in which a low dose of a stressor results in adaptive beneficial effects on cellular function (**Calabrese et al., 2015**; **Rattan, 2008**). Hormesis and the underlying stress-responses that promote longevity converge on cellular pathways, including oxidative stress, insulin signaling, autophagy, and protein homeostasis (**Guo et al., 2022**), to promote longevity.

Multicellular organisms secrete a highly conserved set of neuromodulators, including neurotransmitter and neuropeptide signals from the CNS. These signals integrate information about the organism's external environment and internal state to coordinate a physiological response in peripheral tissues. Within the context of aging, bioamine neurotransmitters contribute to the activation of many well-studied stress response mechanisms that promote longevity. For example, serotonin signaling modulates the mitochondrial unfolded protein response in *Caenorhabditis elegans* (**Prasad and Clark, 2006**) and regulates how food perception contributes to dietary restriction-mediated longevity in worms (**Miller et al., 2022**) and flies (**Libert et al., 2007**). Dopamine also modifies the longevity benefits of dietary restriction in invertebrates (**Miller et al., 2022**; **Kitto et al., 2024**), and polymorphisms in the dopamine D4 receptor are associated with longevity in humans (**Grady et al., 2013**). Finally, adrenaline and its invertebrate analog, tyramine, have been linked to changes in the aging rate in both nematodes (**Kitto et al., 2024**; **Veuthey et al., 2024**; **Özbey et al., 2020**; **De Rosa et al., 2019**) and mammals (**Riera et al., 2014**). Hormone signals such as insulin (**Wolkow et al., 2000**; **Boylston et al., 2006**; **Blüher et al., 2003**), growth factors (**Kappeler et al., 2008**; **Holzenberger et al., 2003**), and GnRH (**Kitto et al., 2024**; **Zhang et al., 2013**) also contribute to longevity pathways across taxa. This growing body of work has led to great interest in manipulating longevity-promoting neural circuits to improve health (**Miller et al., 2020**). While significant research effort focuses on pathways like autophagy, insulin signaling, and proteostasis in the context of aging, the role of hypoxia remains relatively underexplored. Currently, no longevity-promoting agents have been reported to target the hypoxic response.

The hypoxic response is highly conserved across species (**Shen et al., 2005**; **Epstein et al., 2001**; **Kaeberlein and Kapahi, 2009**), highlighting the relevance of this pathway in other organisms, including humans. In *C. elegans*, genetically activating the hypoxic response by knocking down or mutating the E3 ubiquitin ligase von Hippel-Lindau-1 (VHL-1; **Müller et al., 2009**) protein or stabilizing the hypoxia-inducible factor-1 (HIF-1) transcription factor (**Zhang et al., 2009**; **Leiser et al., 2015**) is sufficient to extend lifespan. All these interventions—environmental hypoxia, VHL-1 knockdown, and HIF-1 stabilization—require the intestinal enzyme flavin-containing monooxygenase-2 (*fmo-2*) to extend lifespan in *C. elegans* (**Leiser et al., 2015**). Hypoxic conditions also extend lifespan in a short-lived progeria mouse model (**Rogers et al., 2023**), and epidemiological studies indicate a correlation between hypoxia exposure and longevity (**Li et al., 2017**; **Burtscher, 2014**). However, the physiological changes induced by the hypoxic response are broad and involve adaptations such as increased vascularization, metabolic rewiring, and changes in cell survival pathways. In mammals, some of these same adaptations can be detrimental, as mutations in components of the hypoxic response have been linked to conditions like cancer and cardiovascular disease (**Ohh et al., 2022**; **Wind and Lonser, 2011**; **Lonser et al., 2003**; **Kaelin, 2002**). Additionally, HIF activity is essential to promote some forms of stress resistance to infection (**Vora et al., 2022**; **Nakazawa et al., 2016**) and oxidative stressors (**Bellier et al., 2009**; **Palazon et al., 2014**) but can have detrimental effects on proteostasis (**Fawcett et al., 2015**). This presents a key challenge: while hypoxia-induced longevity in a post-mitotic invertebrate model like *C. elegans* is promising, some of the mechanisms involved may not be directly translatable to mammals without causing deleterious side effects. Therefore, a mechanistic

understanding of the individual cells, neural circuits, and pathways that mediate the beneficial but not detrimental effects of hypoxia on aging is essential to determine whether this circuit could be leveraged to improve human health.

Our previous work in *C. elegans* identified that stabilization of HIF-1 in neurons is sufficient to extend lifespan through the serotonin receptor, SER-7. This pathway eventually leads to the induction of *fmo-2*, a longevity gene expressed in the intestine (***Leiser et al., 2015***; ***Bhat et al., 2024***). In this study, we uncover key neural components of the longevity circuit initiated by genetic induction of the hypoxic response. Within this circuit, we identify individual cells, signals, and receptors necessary and/or sufficient to extend lifespan downstream of genetic activation of the hypoxic response. More specifically, we find serotonin signaling in the ADF serotonergic neurons is both necessary and sufficient to extend lifespan through genetic activation of the hypoxic response. This pathway signals through the serotonin receptor SER-7 in the RIS interneuron. We further demonstrate additional neurotransmitters (GABA and tyramine), and a neuropeptide (NLP-17) are critical for mediating these longevity effects. Finally, we identify that oxygen sensing neurons (URX, AQR, PQR, and BAG) act downstream of neuronal HIF-1 in this circuit. Our insights into this longevity pathway provide a mechanistic understanding of how genetic activation of the hypoxic response delays aging and improves health.

Results

Serotonin signaling through the ADF neuron and the SER-7 receptor are necessary and sufficient for genetic activation of the hypoxic response to extend lifespan

Induction of the hypoxic response by targeted genetic manipulations can increase lifespan in *C. elegans*. These manipulations include decreasing activity of the VHL-1 E3 ubiquitin ligase that targets the transcription factor HIF-1 for degradation under hypoxia (***Müller et al., 2009***) or by a mutation that stabilizes HIF-1 (HIF-1^{P621A}; ***Zhang et al., 2009***; ***Leiser et al., 2015***; ***Figure 1A***). We previously found that stabilizing HIF-1 in serotonergic neurons is sufficient to extend lifespan (***Leiser et al., 2015***). To determine which serotonergic neurons initiate HIF-1-mediated longevity, we generated strains with a nondegradable HIF-1 variant (HIF-1^{P621A}; ***Leiser et al., 2015***; ***Pocock and Hobert, 2008***) expressed under promoters specific to each of *C. elegans'* three primary serotonergic neuron types—the ADF, NSM, and HSN neurons (***Sze et al., 2000***). These transgenic worms were then crossed into the *hif-1* null background to ensure that HIF stabilization in one neuron type could not feedback to modify HIF-1 activity in other cells. When we measured the lifespan of each strain relative to WT and *hif-1* knockout controls, we observed that stabilizing HIF-1 in the ADF or NSM neurons significantly extended lifespan by 26% and 23%, respectively (***Figure 1B and C***). HIF-1 stabilization in the HSN neurons had a smaller effect but significantly extended lifespan by 9% (***Figure 1D***). This result indicates that modifying signaling in any serotonergic neuron is sufficient to induce some level of hypoxic response-mediated longevity. These data suggest that serotonergic neurons can partially substitute for each other to promote longevity in this pathway. In summary, the ADF and/or NSM serotonergic neurons play an essential role in longevity following genetic activation of the hypoxic response.

After identifying this role for ADF and NSM HIF-1 stabilization, we also asked whether genetically activating the hypoxic response also affected healthspan in three different measures of *C. elegans* mobility: pumping rate, thrashing rate, and movement speed. We found that both ADF- and NSM-specific HIF-1 stabilization had no effect on pumping rate in young (day 1 of adulthood) worms. In aged animals (day 12 of adulthood), however, NSM-, but not ADF-, specific HIF-1 stabilization rescued the pumping rate decline in hif-1 knockout compared to WT worms (***Figure 1—figure supplement 1C***). Similarly, NSM-, but not ADF-, specific HIF-1 stabilization rescued the thrashing rate decline in the hif-1 knockout young and aged worms (***Figure 1—figure supplement 1D***). ADF and NSM HIF-1 stabilization also had no effect on average or maximum movement speed at days 1 and 5 of adulthood (***Figure 1—figure supplement 1E and F***). Together, these results indicate that genetic activation of the hypoxic response in NSM neurons but not in the ADF neurons could improve healthspan.

HIF-1 activity also interacts with multiple stress responses, including oxidative stress, proteotoxic stress, and infection (***Bellier et al., 2009***; ***Palazon et al., 2014***; ***Vora et al., 2022***; ***Nakazawa et al., 2016***; ***Fawcett et al., 2015***). To determine whether various components of this pathway affect both longevity and the response to other stressors, and given that serotonin signaling modulates the

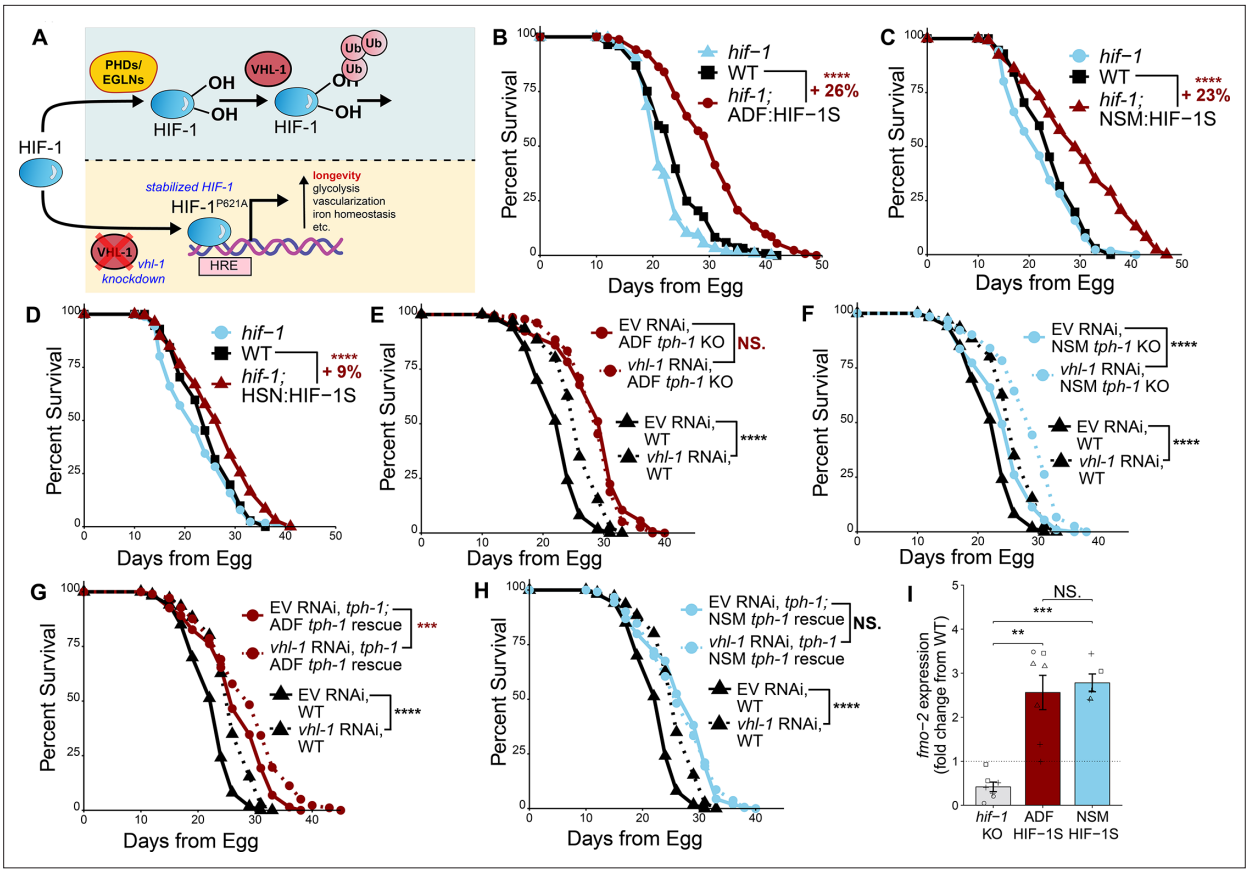


Figure 1. ADF serotonergic neurons are necessary and sufficient to extend lifespan downstream of genetic activation of the hypoxic response. (**A**) Diagram of the conserved hypoxic response and genetic activation of the hypoxic response by *vhl-1* knockdown and HIF-1 stabilization. (**B–D**) Survival curves of WT, *hif-1(ia4)* knockout, *hif-1(ia4);* ADF::HIF-1S (**B**), *hif-1(ia4);* NSM::HIF-1S (**C**), and *hif-1(ia4);* HSN::HIF-1S (**D**) worms. N≥256 (**B**), N≥188 (**C**), and N≥188 (**D**) worms per condition. (**E**) Survival curves of WT and ADF:*tph-1* knockout worms on empty vector (EV) or *vhl-1* RNAi. N≥143 worms per condition. (**F**) Survival curves of WT and NSM:*tph-1* knockout worms on empty vector (EV) or *vhl-1* RNAi. N≥193 worms per condition. (**G**) Survival curves of WT and *tph-1(mg280);* ADF:*tph-1* rescue worms on empty vector (EV) or *vhl-1* RNAi. N≥178 worms per condition. (**H**) Survival curves of WT and *tph-1(mg280);* NSM:*tph-1* rescue worms on empty vector (EV) or *vhl-1* RNAi. N≥160 worms per condition. (**I**) Gene expression of *fmo-2* in WT, *hif-1(ia4)* knockout, *hif-1(ia4);* ADF:HIF-1S, and *hif-1(ia4);* NSM:HIF-1S worms. Significance in panels B–H is from a log-rank test comparing median survival. Significance in panel I is from a Student's t-test. In all panels, three replicates were plotted together, and all statistics include a Bonferroni correction for multiple comparisons. NS=$p > 0.05$, *=$p < 0.05$, **=$p < 0.01$, ***=$p < 0.001$, and ****=$p < 0.0001$.

The online version of this article includes the following source data and figure supplement(s) for figure 1:

Source data 1. Excel file containing the raw data and statistics plotted in ***Figure 1***.

Figure supplement 1. *tph-1* is required for *vhl-1* mediated longevity.

Figure supplement 1—source data 1. Excel file containing the raw data and statistics plotted in ***Figure 1—figure supplement 1***.

mitochondrial unfolded protein response (mt-UPR; ***Berendzen et al., 2016***), we asked whether stabilizing HIF-1 in these serotonergic neurons may also affect the mt-UPR. We found that HIF-1 stabilization in either the ADF or the NSM decreased the expression of *hsp-6* (***Figure 1—figure supplement 1G***), a downstream effector of the mt-UPR (***Haeussler and Conradt, 2022***). This could suggest either that the mt-UPR response is impaired in these worms, or that HIF-1 stabilization decreases proteotoxic stress leading to a lower basal level of *hsp-6*.

To further test the necessity of the most impactful (for lifespan) serotonergic neurons in genetic activation of the hypoxic response-mediated longevity, we used transgenic animals in which *tph-1*, the rate-limiting enzyme in serotonin synthesis, was knocked out exclusively in the ADF or the NSM serotonergic neurons (***Miller et al., 2022***; ***Flavell et al., 2013***). We then measured the lifespans of these strains on empty vector (EV) and *vhl-1* RNAi to determine the necessity of ADF and NSM serotonergic signaling in *vhl-1*-mediated longevity. Throughout this manuscript decreasing *vhl-1* activity to extend

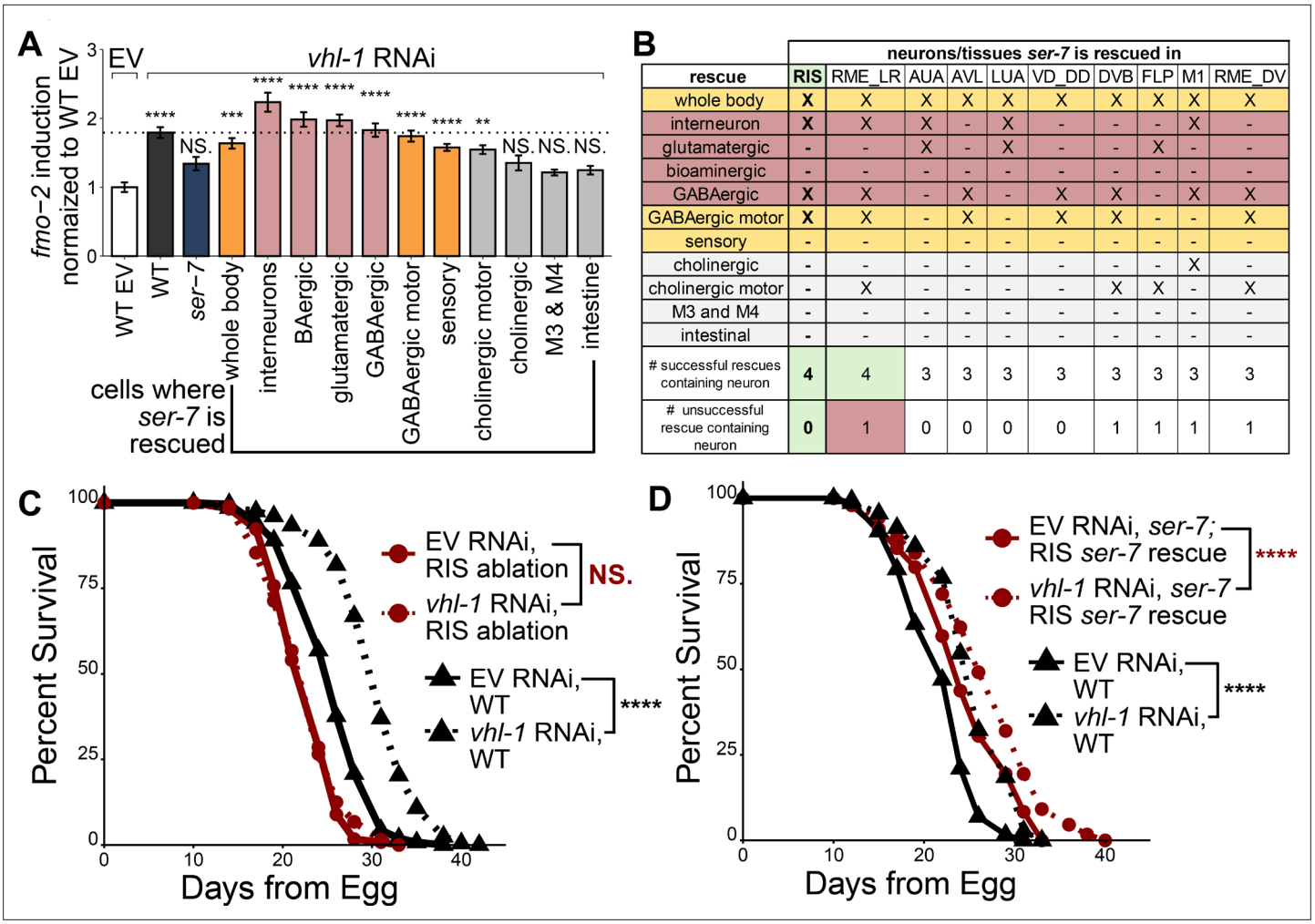
lifespan, either by RNAi knockdown or by genetic knockout, will be referred to as *vhl-1*-mediated longevity. Successful RNAi knockdown was confirmed with qPCR validation (***Figure 1—figure supplement 1A***). We found that serotonin synthesis in ADF but not NSM neurons was required for *vhl-1* knockdown to extend lifespan (***Figure 1E and F***). This indicates that while HIF stabilization in multiple serotonergic neurons can extend lifespan, ADF serotonin signaling is required for lifespan extension in response to *vhl-1* knockdown.

To test if serotonin production in a single neuron type is sufficient for genetic activation of the hypoxic response to extend lifespan, we rescued *tph-1* expression in a *tph-1* null background using promoters specific to the ADF or the NSM neurons (***Miller et al., 2022***). The lifespans of these strains on EV or *vhl-1* RNAi were then measured. As expected and consistent with our previous publication (***Leiser et al., 2015***), the lifespan of the *tph-1* knockout strain was not extended by *vhl-1* knockdown (***Figure 1—figure supplement 1B***). Consistent with the ADF neuron's requirement for *vhl-1*-mediated longevity (***Figure 1E and F***), serotonin synthesis in the ADF neurons was sufficient for *vhl-1* knockdown to extend lifespan, while NSM serotonin synthesis was not (***Figure 1G and H***). The enzyme *fmo-2* is induced in the intestine under hypoxia and is required for lifespan extension by environmental hypoxia, HIF-1 stabilization, and *vhl-1* depletion (***Leiser et al., 2015***). To test whether ADF- or NSM-specific HIF-1 stabilization also induces *fmo-2*, we measured *fmo-2* transcription in this strain using qPCR. We found that ADF and NSM HIF-1 stabilization significantly induced *fmo-2* expression relative to WT controls (***Figure 1I***), suggesting a model in which ADF signaling extends lifespan through the same mechanism as *vhl-1* knockdown and environmental hypoxia. Together, these data indicate that while HIF-1 stabilization in any serotonergic neuron is sufficient to extend lifespan, only ADF serotonin production is necessary and sufficient for *vhl-1*-mediated longevity. This suggests that under normal physiological conditions, the serotonergic ADF neurons propagate a signal in response to whole body stabilized HIF-1.

After identifying ADF neurons as the most central serotonergic neurons in longevity following genetic activation of the hypoxic response, we next sought to determine the downstream receptor responding to serotonin signaling from ADF neurons. *C. elegans* have six known serotonin receptors—SER-1, SER-4, SER-5, SER-7, MOD-1, and LGC-50. Of these six receptors, our previous findings showed that *ser-7* expression is required for *vhl-1* knockdown to induce *fmo-2* and extend lifespan (***Leiser et al., 2015***). SER-7 is a G-protein-coupled receptor (GPCR) with high sequence identity to the 5-HT_7 receptor in mammals (***Hobson et al., 2006***; ***Carre-Pierrat et al., 2006***). *ser-7* is thought to be expressed in 27 of *C. elegans'* 302 neurons (***Taylor et al., 2021***) and contributes to many aspects of physiology, such as reproduction and pharyngeal pumping (***Hobson et al., 2006***). Consequently, broad manipulation of SER-7 signaling is not an ideal method for exclusively modifying aging. To identify more specific targets for lifespan extension within this pathway, we asked whether *ser-7* expression in any subset of neurons is sufficient to rescue the *vhl-1*-mediated *fmo-2* induction in a *ser-7* null background.

We created transgenic strains with *ser-7* expression under the control of 11 different cell-specific promoters in a *ser-7* null background. These promoters were selected to rescue *ser-7* expression in the following neuronal populations: whole-body rescue (*ser-7p::ser-7*), interneuron rescue (*glr-1p::ser-7*), bioaminergic neuron rescue (*cat-1p::ser-7*), glutamatergic neuron rescue (*eat-4p::ser-7*), GABAergic neuron rescue (*unc-47p::ser-7*), cholinergic neuron rescue (*unc-17p::ser-7*), sensory neuron rescue (*osm-6p::ser-7*), GABAergic motor neuron rescue (*unc-25p::ser-7*), cholinergic motor neuron rescue (*acr-2p::ser-7*), M3 and M4 neuron rescue (*ceh-28p::ser-7*), and intestinal rescue (*vha-6p::ser-7*) in a *ser-7* null background. To measure whether *ser-7* expression restores *vhl-1*-mediated longevity, we injected each construct into *ser-7* null worms crossed with a single-copy transcriptional reporter for *fmo-2 (fmo-2p::mCherry*). Because *fmo-2* is induced by and required for hypoxia-mediated longevity (***Leiser et al., 2015***), we utilized its induction as an efficient screening tool to identify components of this longevity pathway.

We first confirmed that *ser-7* knockout attenuates *vhl-1*-mediated *fmo-2* induction (***Figure 2A***). The whole-body rescue of *ser-7* expression under the endogenous *ser-7* promoter restored *fmo-2* induction to 91% of WT controls (***Figure 2A***). Of the 10 cell-specific *ser-7* rescues, expression in interneurons, bioaminergic neurons, glutamatergic neurons, or GABAergic neurons fully rescued *vhl-1*-mediated *fmo-2* induction to ≥100% of the WT control response (***Figure 2A***, pink bars). *ser-7* rescue in GABAergic motor neurons or in sensory neurons showed a partial rescue (defined as a



rescue	neurons/tissues *ser-7* is rescued in									
	RIS	RME_LR	AUA	AVL	LUA	VD_DD	DVB	FLP	M1	RME_DV
whole body	X	X	X	X	X	X	X	X	X	X
interneuron	X	X	X	-	X	-	-	-	X	-
glutamatergic	-	-	X	-	X	-	-	X	-	-
bioaminergic	-	-	-	-	-	-	-	-	-	-
GABAergic	X	X	-	X	-	X	X	-	X	X
GABAergic motor	X	X	-	X	-	X	X	-	-	X
sensory	-	-	-	-	-	-	-	-	-	-
cholinergic	-	-	-	-	-	-	-	-	X	-
cholinergic motor	-	X	-	-	-	-	X	X	-	X
M3 and M4	-	-	-	-	-	-	-	-	-	-
intestinal	-	-	-	-	-	-	-	-	-	-
# successful rescues containing neuron	4	4	3	3	3	3	3	3	3	3
# unsuccessful rescue containing neuron	0	1	0	0	0	0	1	1	1	1

Figure 2. *ser-7* expression in the GABAergic RIS neuron is required for genetic activation of the hypoxic response to extend lifespan. (**A**) Quantification of *fmo-2p::mCherry* (WT positive control), *fmo-2p::mCherry; ser-7(tm1325)* knockout (negative control), and *fmo-2p::mCherry; ser-7(tm1325)* knockouts with *ser-7* rescued in the whole body (*ser-7p::ser-7*), interneurons (*glr-1p::ser-7*), bioaminergic neurons (*cat-1p::ser-7*), glutamatergic neurons (*eat-4p::ser-7*), GABAergic neurons (*unc-47p::ser-7*), GABAergic motor neurons (*unc-25p::ser-7*), sensory neurons (*osm-6p::ser-7*), cholinergic motor neurons (*acr-2p::ser-7*), cholinergic neurons (*unc-17p::ser-7*), M3 and M4 neurons (*ceh-28p::ser-7*), and the intestine (*vha-6p::ser-7*) on empty vector (EV, WT control shown) or *vhl-1* RNAi (all strains shown). Bar height indicates the mean fluorescence on *vhl-1* RNAi of each genotype normalized to the empty vector control value from that genotype. The dashed line indicates the *vhl-1 RNAi*-mediated *fmo-2* induction of WT positive control. N≥45 worms per condition. Error bars indicate SEM. Significance is from a two-way ANOVA (*fmo-2* induction ~genotype x RNAi) and post-hoc Tukey HSD test. Stars signify results from this post-hoc test comparing the *fmo-2* induction of each strain on EV RNAi with the *fmo-2* induction of that strain on *vhl-1* RNAi. (**B**) A table showing the 10 *ser-7* expressing candidate neurons and their expression patterns among the *ser-7* cell-specific strains that successfully rescued *fmo-2* induction in **A**. Pink rows indicate rescues that fully restored *vhl-1* mediated *fmo-2* induction, orange rows indicate rescues that partially restored *vhl-1*-mediated *fmo-2* induction, and gray rows signify unsuccessful rescue constructs from the data in **A**. (**C**) Survival curve of WT and RIS ablation (*Ex[srsx-18p::caspase-3(p12)-nz]; Ex[srsx-18p::cz-caspase-3 (p17)]*; *srsx-18p::GFP*) worms on empty vector (EV) and *vhl-1* RNAi. N≥192 worms per condition. (**D**) Survival curve of WT and *ser-7 (tm1325); ser-7* rescue in the RIS neuron (*flp-11p::ser-7*) worms on EV and *vhl-1* RNAi. N≥144 worms per condition. Significance in panels C and D is from a log-rank test comparing median survival. In all panels, NS=$p > 0.05$, *=$p < 0.05$, **=$p < 0.01$, ***=$p < 0.001$, and ****=$p < 0.0001$. In all panels, three replicates were plotted together, and all statistics include a Bonferroni correction for multiple comparisons.

The online version of this article includes the following source data and figure supplement(s) for figure 2:

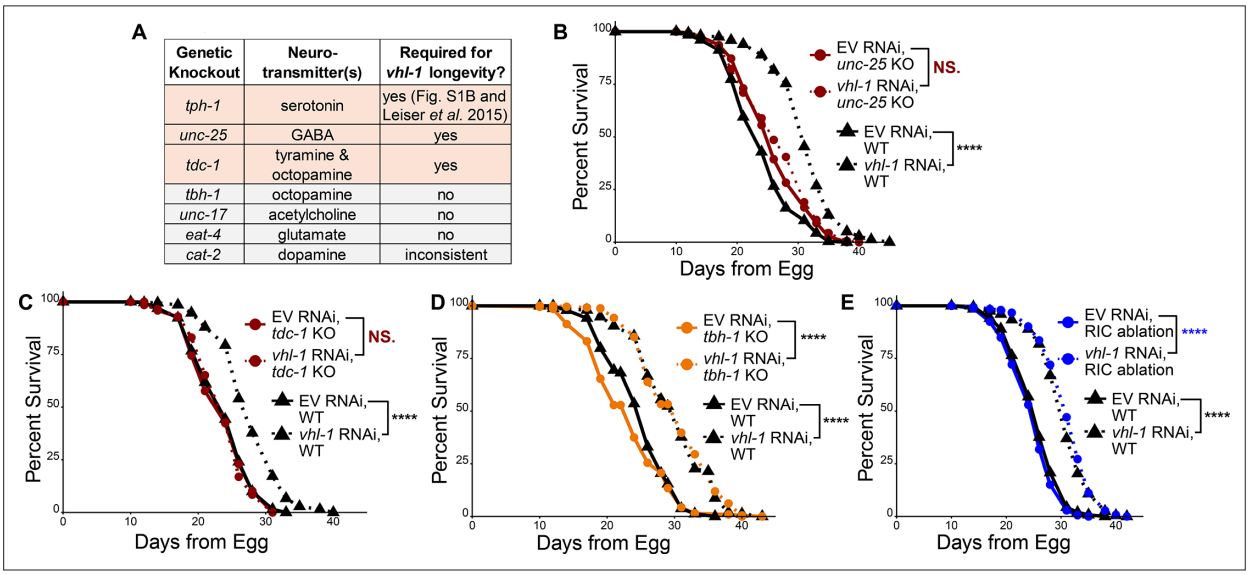
Source data 1. Excel file containing the raw data and statistics plotted in ***Figure 2***, ***Figure 2—figure supplement 1***.

Figure supplement 1. *ser-7* expression in each *ser-7* expressing neuron is rescued by at least one construct, and *ser-7* is required for *vhl-1*-mediated longevity.

50–99% increase from *fmo-2* induction in the *ser-7* knockout; ***Figure 2A***, orange bars). In contrast, rescuing *ser-7* in cholinergic motor neurons, cholinergic neurons, M3 and M4 neurons, or in the intestine did not rescue (***Figure 2A***, gray bars). Taken together, 6 of the 10 cell-specific *ser-7* rescues at least partially restored *vhl-1*-mediated *fmo-2* induction, including some that have no known overlap in *ser-7* expression patterns. Collectively, these data suggest that serotonin receptor *ser-7* expression in multiple neurons may be sufficient to convey the hypoxic signal to the intestine and induce *fmo-2*.

We compiled a table containing the top candidates for the *ser-7* neuron based on which rescue constructs restored *ser-7* expression (simplified table in ***Figure 2B***, full table in ***Figure 2—figure supplement 1A***). We hypothesized that neurons present in many of the successful rescue constructs would be most important in the *vhl-1*-mediated longevity circuit. Conversely, we hypothesized that candidate neurons within rescues that did not restore a WT-like response are less likely to be important (***Figure 2B***; ***Figure 2—figure supplement 1A***). We acknowledge that this analysis strategy is biased toward neurons rescued in a greater proportion of the transgenic strains, which could lead to false negatives. From this analysis, we identified 10 neurons that were rescued in 3–4 of the 6 successful rescue constructs (***Figure 2B***). Five of these neurons (DVB, FLP, M1, RME_LR, and RME_DV) were also present in unsuccessful rescue constructs, so they were not considered for follow-up experiments. Of the remaining five neurons (RIS, AUA, AVC, LUA, and VD_DD), the top candidate was the RIS neuron, because RIS was present in the highest number (4 as shown in ***Figure 2B***) of successful rescue constructs.

To validate whether the RIS neuron is a key signaling cell in *vhl-1*-mediated longevity, we first genetically ablated the RIS neuron to test its necessity. Our results showed that *vhl-1* RNAi does not extend lifespan of RIS ablated worms, indicating that the RIS neuron is completely required for *vhl-1* knockdown to extend lifespan (***Figure 2C***). To test the sufficiency of RIS signaling, we next rescued *ser-7* expression in the RIS neuron in the *ser-7* null background under the *flp-11* promoter. *flp-11* is expressed in the RIS neuron (***Turek et al., 2016***) and uv1 neuroendocrine cells (***Banerjee et al., 2017***) that do not endogenously express *ser-7* (***Taylor et al., 2021***). We first confirmed that *ser-7* knockout



Genetic Knockout	Neuro-transmitter(s)	Required for *vhl-1* longevity?
tph-1	serotonin	yes (Fig. S1B and Leiser *et al.* 2015)
unc-25	GABA	yes
tdc-1	tyramine & octopamine	yes
tbh-1	octopamine	no
unc-17	acetylcholine	no
eat-4	glutamate	no
cat-2	dopamine	inconsistent

Figure 3. GABA and tyramine synthesis are required for *vhl-1* knockdown to extend lifespan. (**A**) Summary table of the necessity of each *C. elegans* neurotransmitter for *vhl-1* RNAi-mediated longevity. (**B–E**) Survival curves of WT and *unc-25(e156)* (GABA deficiency) (**B**), *tdc-1(n3419)* (tyramine and octopamine deficiency) (**C**), *tbh-1(n3247)* (octopamine deficiency) (**D**), and RIC ablation (*Ex[tbh-1p::caspase-3(p12)-nz]; Ex[tbh-1p::cz-caspase-3 (p17)]*; *tbh-1p::GFP*) (**E**) worms on empty vector (EV) and *vhl-1* RNAi. N≥310 (**B**), ≥201 (**C**), ≥258 (**D**), and ≥258 (**E**) worms per condition. Significance in panels B–E is from a log-rank test comparing median survival. NS=$p > 0.05$, *=$p < 0.05$, **=$p < 0.01$, ***=$p < 0.001$, and ****=$p < 0.0001$. In all panels, three replicates were plotted together, and all statistics include a Bonferroni correction for multiple comparisons.

The online version of this article includes the following source data and figure supplement(s) for figure 3:

Source data 1. Excel file containing the raw data and statistics plotted in ***Figure 3***.

Figure supplement 1. Acetylcholine, glutamate, and dopamine synthesis are not fully required for *vhl-1* RNAi to extend lifespan.

Figure supplement 1—source data 1. Excel file containing the raw data and statistics plotted in ***Figure 3—figure supplement 1***.

worms are partially required for *vhl-1* RNAi to extend lifespan (***Figure 2—figure supplement 1B***, Cox Regression, p=0.003, **). Significantly, *ser-7* rescue in the RIS neuron (*ser-7; flp-11p::ser-7*) restores the lifespan extension by *vhl-1* RNAi to the same degree as WT worms (***Figure 2D***). These data suggest that *ser-7* expression in the RIS neuron only is sufficient for *vhl-1*-mediated longevity. However, one limitation of this approach is that non-physiological expression of *ser-7* in the uv1 cells could play a role in restoration of WT-like *vhl-1*-mediated *fmo-2* induction. Together, these data are consistent with a model where genetic activation of the hypoxic response stabilizes HIF-1 in the ADF neurons, which modifies serotonin signaling to the SER-7 receptor on the RIS interneuron.

Tyraminergic signaling from the RIM neuron and the tyramine receptor TYRA-3 are required for *vhl-1* knockdown to extend lifespan

After identifying neuron subtypes involved in serotonin signaling downstream of genetic activation of the hypoxic response, we next set out to identify whether other neurotransmitters act in the pathway. To answer this question, we obtained mutants deficient in the production of each type of neurotransmitter in *C. elegans* (***Figure 3A***) and measured their lifespan on control and *vhl-1* RNAi. Out of the six neurotransmitters we tested, blocking the production of GABA (*unc-25*, ***Figure 3B***) or tyramine and octopamine (*tdc-1*, ***Figure 3C***) attenuated longevity on *vhl-1* RNAi. The requirement of GABA is consistent with our finding that *ser-7* expression on the GABAergic RIS neuron is also necessary for *vhl-1*-mediated longevity (***Figure 2***), connecting the serotonergic and GABAergic components of this circuit.

Tyramine (analogous to mammalian adrenaline, ***Bauknecht and Jékely, 2017***) is synthesized from tyrosine by tyrosine decarboxylase (*tdc-1*) and can be further converted to octopamine (analogous to mammalian noradrenaline) by tyramine β-hydroxylase (*tbh-1*) in *C. elegans* (***Alkema et al., 2005***). Therefore, the *tdc-1* knockout is deficient in both tyramine and octopamine synthesis (***Figure 3C***) and the *tbh-1* knockout (***Figure 3D***) is only deficient in octopamine synthesis. Since worms lacking only octopamine (*tbh-1*, ***Figure 3D***) were long-lived on *vhl-1* RNAi but worms lacking both tyramine and octopamine (*tdc-1*, ***Figure 3C***) were not, we can conclude that tyramine is required for genetic activation of the hypoxic response to extend lifespan. To further test whether tyramine but not octopamine is involved in this pathway, we generated a strain in which the primary octopamine-producing neuron, RIC (***Alkema et al., 2005***), is genetically ablated. We found that the RIC neuron is not required for *vhl-1*-mediated longevity (***Figure 3E***), further supporting that tyramine but not octopamine is a key neurotransmitter in the circuit driving longevity after genetic activation of the hypoxic response.

In addition to octopamine (*tbh-1*, ***Figure 3—figure supplement 1C***), we also observed that acetylcholine (*unc-17*, ***Figure 3—figure supplement 1A***) and glutamate (*eat-4*, ***Figure 3—figure supplement 1B***) were not required for lifespan extension by *vhl-1* RNAi. Our lifespans of the dopamine

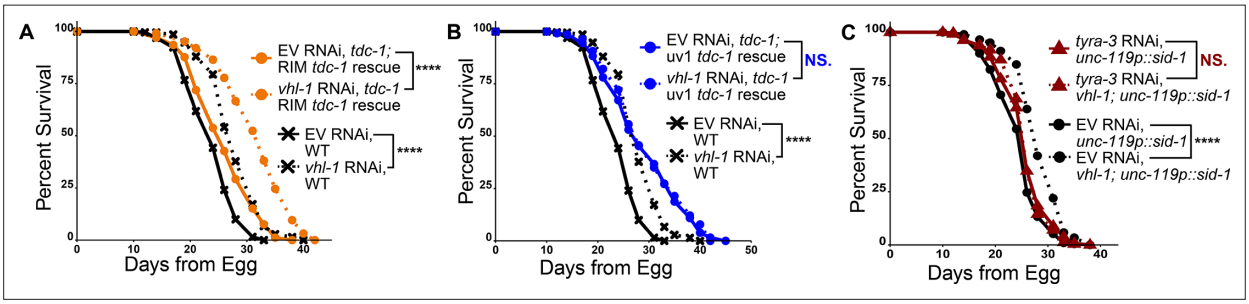


Figure 4. The RIM neuron and the tyramine receptor *tyra-3* act in the *vhl-1* RNAi-mediated longevity pathway. (**A, B**) Survival curves of WT, RIM rescue (*tdc-1 (n3419);* Ex[*ocr-4p::tdc-1]*) (**A**), and uv1 *tdc-1* rescue (*tdc-1 (n3419);* Ex[*gcy-13p::tdc-1]*) (**B**) strains on empty vector (EV) and *vhl-1* RNAi. N≥126 (**A**) and N≥140 (**B**) worms per condition. (**C**) Survival curves of TU3311(*unc-119p::sid-1*) and *vhl-1(ok161)*; TU3311(*unc-119p::sid-1*) worms on empty vector (EV) and *tyra-3* RNAi. N≥215 worms per condition. Significance in all panels is from a log-rank test comparing median survival. NS=$p > 0.05$, *=$p < 0.05$, **=$p < 0.01$, ***=$p < 0.001$, and ****=$p < 0.0001$. In all panels, three replicates were plotted together, and all statistics include a Bonferroni correction for multiple comparisons.

The online version of this article includes the following source data and figure supplement(s) for figure 4:

Source data 1. Excel file containing the raw data and statistics plotted in ***Figure 4***.

Figure supplement 1. *tyra-2* and *ser-2* are not necessary for *vhl-1*-mediated longevity, while *lgc-55* is partially required.

synthesis mutant *cat-2* indicated that dopamine is inconsistently required for genetic activation of the hypoxic response to extend lifespan. In three biological replicates, we observed a full requirement, partial requirement, and no requirement for dopamine synthesis in *vhl-1* RNAi-mediated longevity. When analyzed together, the net result suggests that dopamine is partially required for *vhl-1*-mediated longevity (***Figure 3—figure supplement 1C***, Cox Regression for interaction between genotype and *vhl-1* RNAi, $p<0.0001$, ****). We did not follow up on dopamine due to the inconsistency. Together, the results from this neurotransmitter screen support the conclusion that in addition to serotonin, both GABA and tyramine play a role in *vhl-1*-mediated longevity.

Nematodes synthesize GABA in 26 of 302 neurons while tyramine is only synthesized in two cells (***Hobert, 2013***). As a result, identifying highly specific components of tyraminergic signaling is more feasible than mapping GABAergic signaling components. Therefore, we sought to determine the tyramine-producing neuron(s) and tyramine receptor(s) that contribute to *vhl-1*-mediated longevity. In *C. elegans*, the two canonically tyraminergic cell types (the RIM neuron and the uv1 neuroendocrine cells) express *tdc-1* but not *tbh-1* (***Hobert, 2013***). To determine which tyraminergic cell(s) act in the *vhl-1*-mediated longevity pathway, we expressed *tdc-1* under promoters specific to either RIM or uv1 in a *tdc-1* null background (***Kitto et al., 2024***). We then measured whether the lifespans of these tyramine rescue strains could be extended by *vhl-1* RNAi. Our results showed that *vhl-1* RNAi extended lifespan in the RIM rescue strain (***Figure 4A***), but not in the uv1 rescue (***Figure 4B***). This finding demonstrates that tyramine synthesis in the RIM neuron is sufficient for *vhl-1* RNAi to extend lifespan. Notably, both tyramine rescue constructs lived longer than WT controls (***Figure 4A and B***). This could indicate that altering tyramine signaling modifies lifespan both within and independently of the *vhl-1*-mediated longevity pathway.

To identify the tyramine receptor(s) necessary for genetic activation of the hypoxic response to extend lifespan we used RNAi to knock down each of *C. elegans'* four known tyramine receptors (***Rex et al., 2004***; ***Pirri et al., 2009***; ***Wragg et al., 2007***; ***Rex et al., 2005***; ***Figure 4C***). Since tyramine receptors are mostly expressed in neurons, and RNAi uptake into some neurons is less efficient than other cell types, we used a strain with enhanced neuronal RNAi uptake (TU3311, *unc-119p::sid-1*) crossed into *vhl-1* knockout worms. This neural enhanced RNAi uptake strain was not used previously in this work for *vhl-1* RNAi experiments because *vhl-1* RNAi knockdown extends lifespan in WT worms (***Leiser et al., 2015***). The generated *vhl-1; unc-119p::sid-1* strain was long-lived compared to the control strain *unc-119p::sid-1* (***Figure 4C***). Successful RNAi knockdown was validated via qPCR (***Figure 4—figure supplement 1A***). Our lifespan results show that the tyramine receptor *tyra-3* was fully required for *vhl-1*-mediated longevity (***Figure 4C***), but the tyramine receptors *tyra-2* and *ser-2* were not (***Figure 4—figure supplement 1B and C***). Another tyramine receptor, *lgc-55*, showed a partial requirement for *vhl-1*-mediated longevity (***Figure 4—figure supplement 1D***). Although there was a minor lifespan extension by *vhl-1* knockout on *lgc-55* RNAi (***Figure 4—figure supplement 1D***), we did observe a significant interaction between *lgc-55* knockdown and genotype on lifespan (Cox Regression, $p<0.0001$, ****), indicating a partial requirement. In summary, these data indicate that tyramine signaling from the RIM neuron to the TYRA-3 receptor is required for *vhl-1*-mediated longevity, while the LGC-55 receptor may play a partial role. Interestingly, TYRA-3 is highly expressed on the low oxygen/high carbon dioxide-sensing BAG neuron as well as in the intestine (***Taylor et al., 2021***; ***De Rosa et al., 2019***; ***Zimmer et al., 2009***), the site of *fmo-2* induction during hypoxia (***Leiser et al., 2015***).

Oxygen and carbon dioxide sensing neurons act downstream of serotonin signaling

Given that *tyra-3* is highly expressed in the canonical low-oxygen sensing neuron BAG (***Taylor et al., 2021***), we next explored whether neurons responsible for sensing high- and low-oxygen conditions are essential for genetic activation of the hypoxic response to extend lifespan. *C. elegans* have four oxygen sensory neurons: the URX, PQR, and AQR neurons detect high levels of oxygen (***Zimmer et al., 2009***), the BAG neuron responds to low levels of oxygen (***Bretscher et al., 2011***) and high levels of carbon dioxide (***Hallem and Sternberg, 2008***; ***Figure 5A***). We hypothesized that these oxygen sensing cells may perceive hypoxic conditions and help initiate the hypoxic response. Alternatively, these oxygen sensing neurons could modify behavior in response to hypoxia but not play a role in longevity. We found that *vhl-1* knockdown was unable to extend lifespan when we genetically ablated

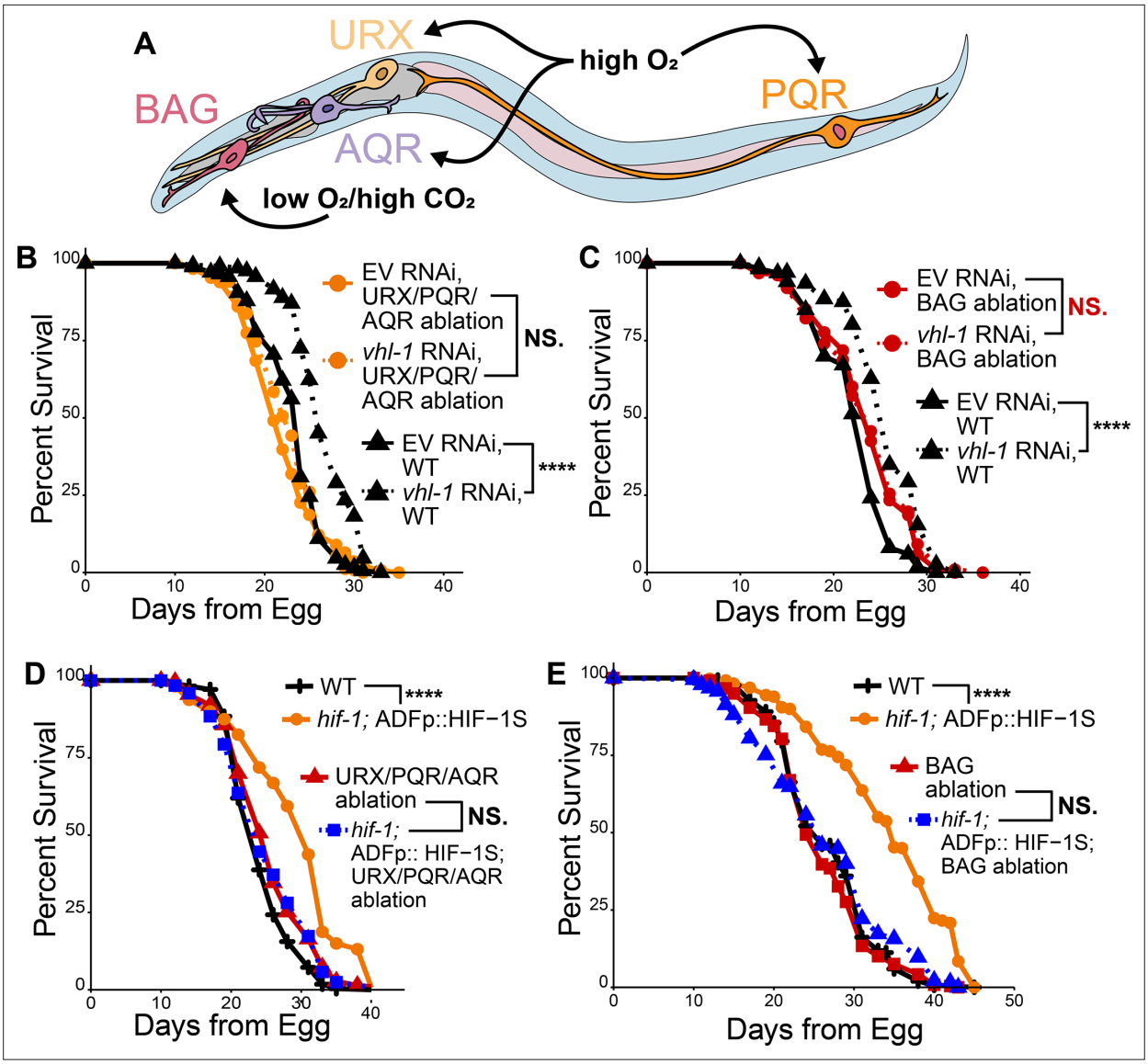


Figure 5. High- and low-oxygen sensing neurons are necessary for genetic activation of the hypoxic response to extend lifespan. (**A**) Diagram of oxygen sensing neurons in *C. elegans*. (**B**) Survival curves of WT and URX/PQR/AQR ablated worms (*qaIs2241 [gcy-36::egl-1+gcy-35::GFP +lin-15(+)]*) on empty vector (EV) and *vhl-1* RNAi. N≥279 worms per condition. (**C**) Survival curves of WT and BAG ablated worms (*Ex[gcy-31p::caspase-3(p12)-nz]; Ex[gcy-31p::cz-caspase-3 (p17)]; gcy-31p::GFP*) on empty vector (EV) and *vhl-1* RNAi. N≥188 worms per condition. (**D**) Survival curves of WT, *hif-1(ia4);* ADF-HIF-1S, URX/PQR/AQR (*qaIs2241 [gcy-36::egl-1+gcy-35::GFP +lin-15(+)]*) ablation, and URX/PQR/AQR (*qaIs2241 [gcy-36::egl-1+gcy-35::GFP +lin-15(+)]*) ablation; *hif-1(ia4);* ADF-HIF-1S worms. N≥150 worms per condition. (**E**) Survival curves of WT, *hif-1(ia4);* ADF-HIF-1S, BAG (*Ex[gcy-31p::caspase-3(p12)-nz]; Ex[gcy-31p::cz-caspase-3 (p17)]; gcy-31p::GFP*) ablation, and BAG (*Ex[gcy-31p::caspase-3(p12)-nz]; Ex[gcy-31p::cz-caspase-3 (p17)]; gcy-31p::GFP*) ablation; *hif-1(ia4);* ADF-HIF-1S worms. N≥186 worms per condition. Significance in all panels is from a log-rank test comparing median survival. NS=$p > 0.05$, *=$p < 0.05$, **=$p < 0.01$, ***=$p < 0.001$, and ****=$p < 0.0001$. In all panels, three replicates were plotted together, and all statistics include a Bonferroni correction for multiple comparisons.

The online version of this article includes the following source data for figure 5:

Source data 1. Excel file containing the raw data and statistics plotted in ***Figure 5***.

the three high-oxygen sensing neurons (URX, AQR, and PQR, ***Figure 5B***). Interestingly, the low O_2/high CO_2 responsive BAG neurons were also required for *vhl-1*-mediated longevity (***Figure 5C***). To test the epistasis of oxygen sensing neurons and serotonergic neurons in this circuit, we next crossed the URX/AQR/PQR ablation worms or BAG ablation worms into *C. elegans* with HIF-1 stabilized in the ADF neurons. Ablation of either the URX/PQR/AQR or the BAG neurons abrogated lifespan extension

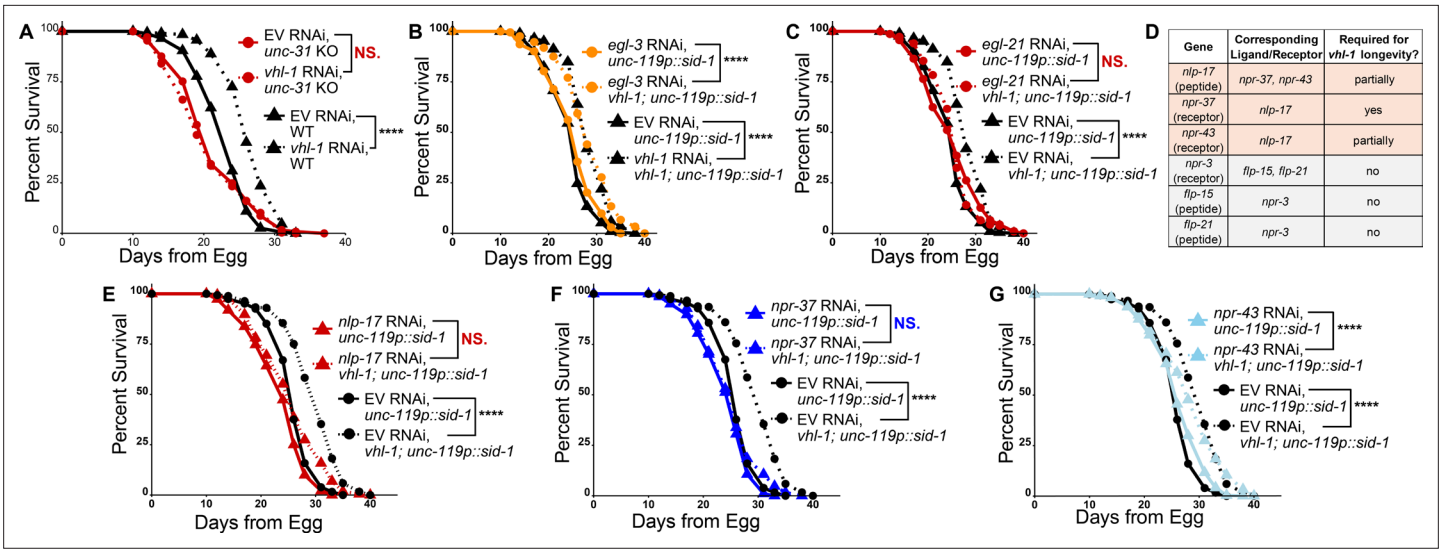


Figure 6. The neuropeptide *nlp-17* and its receptors *npr-37* and *npr-43* are required for *vhl-1*-mediated longevity. (**A**) Survival curves of *unc-31(e169)* and WT worms on empty vector (EV) and *vhl-1* RNAi. N≥242 worms per condition. (**B, C**) Survival curves of TU3311 (*unc-119p::sid-1)* and *vhl-1(ok161);* TU3311 (*unc-119p::sid-1)* worms on empty vector (EV) and *egl-3* (**B**) or *egl-21* (**C**) RNAi. N≥209 worms (**B**) and N≥185 worms (**C**) per condition. (**D**) Summary table of two sets of neuropeptide ligands/receptors that blunted *vhl-1*-mediated lifespan. (**E–G**) Survival curves of TU3311 (*unc-119p::sid-1)* and *vhl-1(ok161);* TU3311 (*unc-119p::sid-1)* worms on empty vector (EV) and *npr-37* (**E**), *npr-43* (**F**), or *nlp-17* (**G**) RNAi. N≥288 worms (**E**), N≥309 worms (**F**), and N≥309 worms (**G**) per condition. Significance in panels A-C and E-G are from log-rank test comparing median survival. Cox Regression for a significant interaction between *npr-43* knockdown and *vhl-1* knockout on lifespan, $p<0.01$, **. Cox regression for a significant interaction between *nlp-17* knockdown and *vhl-1* knockout on lifespan, $p<0.05$, *. NS=$p > 0.05$, *=$p < 0.05$, **=$p < 0.01$, ***=$p < 0.001$, and ****=$p < 0.0001$. In all panels, three replicates were plotted together, and all statistics include a Bonferroni correction for multiple comparisons.

The online version of this article includes the following source data and figure supplement(s) for figure 6:

Source data 1. Excel file containing the raw data and statistics plotted in ***Figure 6***.

Figure supplement 1. qPCR validation of RNAi hits from ***Figures 5 and 6***, and neuropeptide screen hits that did not validate.

Figure supplement 1—source data 1. Excel file containing the raw data and statistics plotted in ***Figure 6—figure supplement 1***.

in the ADF HIF-1 stabilized worms. This suggests that oxygen sensing neurons act downstream of ADF HIF-1 stabilization in this pathway (***Figure 5D and E***).

The neuropeptide NLP-17 and its receptors contribute to *vhl-1*-mediated longevity

After identifying neurons, neurotransmitters, and neuroreceptors acting in the *vhl-1*-mediated longevity circuit, we wondered how this neural circuit ultimately propagates information about hypoxic conditions to the intestine and induces the pro-longevity gene *fmo-2*. The *C. elegans* nervous system does not directly innervate the intestine. Instead, neurosignaling molecules bind to receptors on peripheral tissues through packaging in dense-core vesicles and subsequent release into and diffusion through pseudocoelomic fluid (***Davanian et al., 2019***; ***Li and Kim, 2008***). These dense-core vesicles are packaged with a wide variety of neuropeptide signals, although there is also evidence that bioaminergic neurotransmitters like serotonin, dopamine, and adrenaline/noradrenaline can also signal through this dense-core vesicle mechanism (***Noble et al., 2013***; ***Speese et al., 2007***; ***Palamiuc et al., 2017***).

We first tested if inducing the hypoxic response through *vhl-1* RNAi extends lifespan in a mutant strain lacking the dense-core vesicle packaging gene *unc-31*. We observed that *unc-31* was required for *vhl-1* knockdown to extend lifespan (***Figure 6A***). To examine whether neuropeptide signals carried by dense-core vesicles are involved, we knocked down two neuropeptide processing enzymes—*egl-3* and *egl-21* (***Li and Kim, 2008***). Successful knockdown was validated with qPCR (***Figure 6—figure supplement 1A***). Interestingly, *egl-21* but not *egl-3* was required for *vhl-1* -mediated longevity (***Figure 6B and C***). This could be because *egl-21* is the only enzyme known to perform the carboxypeptidase E cleavage step of neuropeptide processing (***Jacob and Kaplan, 2003***), while there are

four known proprotein convertases with similar function to *egl-3* (***Li and Kim, 2008***; ***Thacker and Rose, 2000***).

We next tested a group of six genes corresponding to neuropeptide/receptor binding pairs that blunted *vhl-1* -mediated *fmo-2* induction (***Figure 6D***). These genes, along with their corresponding receptors, were targeted for RNAi and tested for lifespan in TU3311 (*unc-119p::sid-1*) and TU3311 (*unc-119p::sid-1*); *vhl-1 (ok161)* strains. We found that the *npr-3* receptor and its ligands, *flp-15* and *flp-21*, were not required for *vhl-1*-mediated longevity (***Figure 6—figure supplement 1***). However, knocking down the neuropeptide *nlp-17* partially blocked *vhl-1*-mediated longevity (***Figure 6E***, Cox regression $p<0.05$). Consistently, knocking down *nlp-17's* receptors also completely (*npr-37*, ***Figure 6F***) or partially (*npr-43*, ***Figure 6G***, Cox regression $p<0.001$) blocked *vhl-1*-mediated longevity. Successful knockdown of *npr-37* and *npr-43* was validated with qPCR (***Figure 6—figure supplement 1***). The *nlp-17* RNAi result was validated using a genetic knockout (*nlp-17 (ok3461)*), which completely prevented *vhl-1* knockdown from extending lifespan (***Figure 6—figure supplement 1***). To test whether *nlp-17* acts downstream of other signals in this circuit, we measured the expression of *nlp-17* in ADF- and NSM-specific HIF-1 stabilized strains. Compared to WT and *hif-1* KO controls, we observed no change in *nlp-17* expression when HIF-1 was stabilized in the ADF or NSM serotonergic neurons (***Figure 6—figure supplement 1***). This could suggest that *nlp-17* signaling may act in parallel to serotonergic signaling following genetic activation of the hypoxic response. Alternatively, neuronal HIF-1 stabilization may modify *nlp-17* splicing or translation without resulting in detectable differences in mRNA levels. Together, these data indicate NLP-17 signaling is required for longevity following genetic activation of the hypoxic response, although whether this peptide is synthesized or released in response to hypoxic response remains unclear.

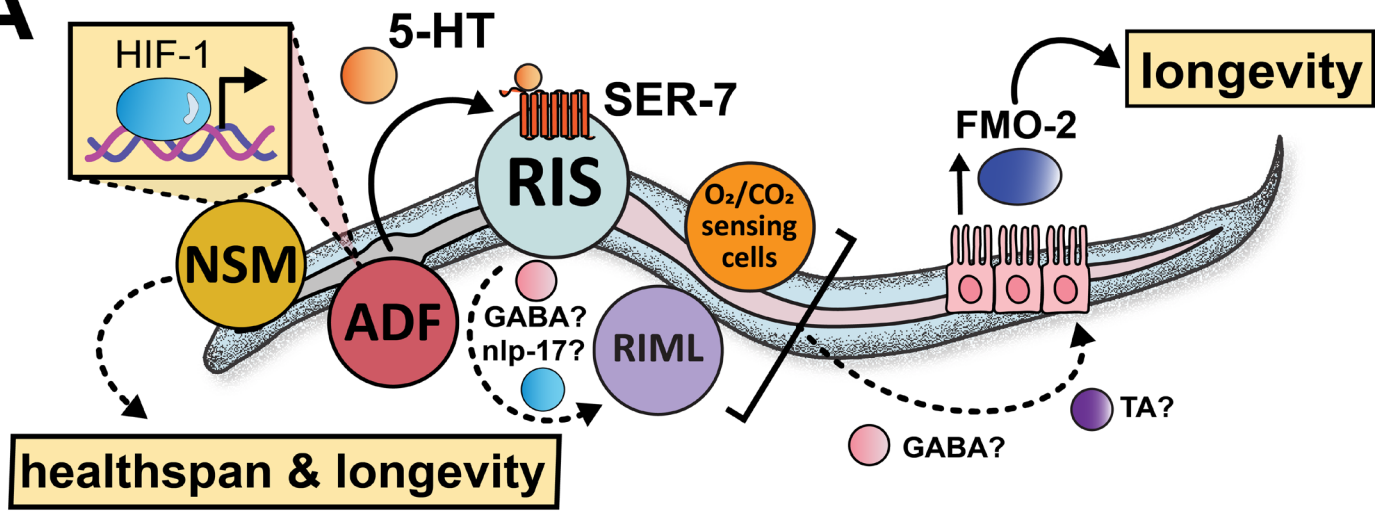
Taken together, these results support a model in which HIF-1 stabilization in the ADF serotonergic neurons leads to modified serotonin signaling from the ADF to the SER-7 expressing and GABA-producing RIS neuron (***Figure 7A and B***). Oxygen sensing neurons act downstream of HIF-1 stabilization in the ADF neuron in this longevity circuit. Tyramine produced by the RIM neuron and neuropeptide (NLP-17) signaling are also required for genetic activation of the hypoxic response to extend lifespan, although it remains unclear whether these signals act upstream, downstream, or in parallel to the serotonergic and GABAergic components in this pathway.

Discussion

In this study, we interrogated a complex signaling pathway through which genetic induction of the hypoxic response extends lifespan in *C. elegans*. Within this pathway, we demonstrate that: (1) stabilization of HIF-1 in the ADF serotonergic neurons modifies signaling to the SER-7 receptor on the GABAergic and neuropeptidergic RIS neuron (***Figures 1 and 2***); (2) tyraminergic signaling through the RIM neuron and the TYRA-3 receptor (***Figures 3 and 4***) are required for *vhl-1*-mediated longevity; (3) oxygen and carbon-dioxide sensory neurons act downstream of HIF-1 stabilization and serotonergic ADF neurons to extend lifespan (***Figure 5***); and (4) in addition to neurotransmitter signals, the neuropeptide NLP-17 and its receptors NPR-37 and NPR-43 are required for genetic activation of the hypoxic response to extend lifespan (***Figure 6***). Ultimately, these neural signals converge on the intestine to activate FMO-2 and extend lifespan (working model summarized in ***Figure 7***). Evidence for the necessity, sufficiency, and epistatic relationships between each signal are summarized in ***Figure 7B***. In brief, all signaling molecules presented in this work are necessary for *vhl-1* depletion to extend lifespan. Rescuing ADF serotonin production, RIS *ser-7* expression, and RIM tyramine production is sufficient for *vhl-1* depletion to extend lifespan. The sufficiency of oxygen sensing neurons BAG and URX/PQR/AQR, and the neuronal signals of GABA, NLP-17, and TYRA-3 to restore *vhl-1*-mediated longevity remains unclear. All of these signals act downstream of *vhl-1* in the hypoxic response-mediated longevity pathway. ADF HIF-1 stabilization and SER-7 signaling act upstream of *fmo-2* induction, and the oxygen sensing neurons (BAG, URX/PQR/AQR) act upstream of or in parallel to ADF HIF-1 stabilization.

The hypoxic response is highly conserved across species, highlighting the potential relevance of this pathway in other organisms, including humans. In nematodes, activating the hypoxic response promotes health and longevity. However, the physiological changes induced by the hypoxic response are broad and involve adaptations that can drive tumorigenesis in mammals. Therefore, a mechanistic understanding of the individual cells, signals, and circuits that mediate the beneficial effects of

A



B

Cell/Signal/ Receptor	Necessary for *vhl-1* depletion to extend lifespan?	Sufficient for *vhl-1* depletion to extend lifespan?	Can manipulating the signal extend lifespan independently of *vhl-1* depletion?	Epistasis in relation to other pathway components?
ADF serotonin production	yes (**Fig. 1E**)	yes (**Fig. 1G**)	yes (**Fig. 1B**)	downstream of *vhl-1* KD (**Fig. 1E**) upstream of *fmo-2* (**Fig. 1I**)
RIS SER-7 expression	likely; RIS neuron is necessary (**Fig. 2C**) but RIS-specific *ser-7* knockout not tested	yes (**Fig. 2D**)	yes (Busack *et al.*, 2023, ref. 79)	downstream of *vhl-1* KD (**Fig. 2C-D**) upstream of *fmo-2* (**Fig. 2A-B**)
GABA	yes (**Fig. 3B**)	unknown	unknown	downstream of *vhl-1* KD (**Fig. 3B**)
RIM tyramine production	likely; *tdc-1* expression is necessary (**Fig. 3C**) but RIM-specific *tdc-1* knockout not tested	yes (**Fig. 4A**)	unknown	downstream of *vhl-1* KD (**Fig. 3C, 4A**)
TYRA-3 receptor	yes (**Fig. 4C**)	unknown	unknown	downstream of *vhl-1* KD (**Fig. 4C**)
BAG & URX/ PQR/AQR neurons	yes (**Fig. 5B-C**)	unknown	unknown	upstream or in parallel to ADF HIF-1 stabilization (**Fig. 5D-E**)
NLP-17 & NPR -37 receptor	yes (**Fig. 6E, G**)	unknown	unknown	downstream of *vhl-1* depletion (**Fig. 6E, G**)

Figure 7. Working model of longevity following genetic activation of the hypoxic response. (**A**) Schematic of working model. (**B**) Table summarizing the necessity, sufficiency, and epistasis of neural signaling components of the working model.

hypoxia is essential. In this work, the discovery that HIF-1 stabilization in the ADF neurons extends lifespan by 26% demonstrates the potential for targeted manipulations within this pathway to have large effects on lifespan. Additionally, our data identify a previously unknown role for tyramine/adrenaline in genetic activation of the hypoxic response as well as establish NLP-17, a neuropeptide with no previous known function, as a signal in *vhl-1*-mediated longevity. This work also demonstrates that the

oxygen sensing AQR, PQR, URX, and BAG neurons act downstream of the serotonergic ADF neuron in genetic activation of the hypoxic response, indicating an interaction between internal and external oxygen sensing mechanisms in longevity. Together, the mapping of these cells, signaling molecules, and receptors acting downstream of genetic activation of the hypoxic response lays the foundation to discover druggable targets that selectively modulate aging in humans without negative side effects.

Other studies in *C. elegans* have also identified neural networks involving the hypoxic response. For example, previous work found a role for HIF-1 in hypoxia-mediated behaviors, such as food-dependent hyperoxia (excessive oxygen) avoidance (***Chang and Bargmann, 2008***). Hyperoxia avoidance requires HIF-1 expression both in the neurons and the tyraminergic uv1 neuroendocrine cells. Interestingly, serotonin signaling from the ADF neuron is also required for WT-like hyperoxia avoidance (***Chang and Bargmann, 2008***). While this HIF-1-mediated behavioral circuit has parallels with the HIF-1-mediated longevity circuit interrogated in this work, these pathways do diverge: the key tyraminergic cell type implicated in hyperoxia avoidance is the uv1 gonadal neuroendocrine cells, while the RIM tyraminergic neurons played a role in longevity (***Figure 4***). Together, the partial overlap between this behavioral and longevity circuit implies that modifying neural signaling to induce the hypoxic response and extend lifespan may also alter behavioral phenotypes. Future research in this area should interrogate exactly where these and any other HIF-1-mediated circuits overlap and diverge.

While this study identifies many neural signals required for *vhl-1* knockdown or knockout to extend lifespan, one key limitation of this work is the potential differences between genetic and environmental methods of inducing the hypoxic response. While *vhl-1* knockdown or knockout leads to HIF-1 stabilization by blocking its proteasomal degradation, it also results in hydroxylated but stable HIF-1. This contrasts with environmental hypoxia, in which HIF-1 remains stable because it cannot be hydroxylated. While HIF-1 is stabilized and localized to the nucleus in both cases, there are differences in transcriptional outcomes between stable hydroxylated and unhydroxylated states (***Powell-Coffman and Coffman, 2010***; ***Kruempel et al., 2020***). Additionally, we did not explore the effects of alternative genetic activators of the hypoxic response such as HIF-1 hydroxylase PHD/EGL mutants, which may provide further insight into how different manipulations of the hypoxic response impact longevity. Future work should interrogate the similarities and differences between the circuits driving longevity in response to environmental hypoxia, *vhl-1* knockdown, HIF-1 stabilization, and PHD/EGL knockdown.

The circuit-mapping approaches employed in this work are also impacted by limitations in cell-specific genetic modifications and in the use of RNAi knockdown. For example, cell-specific rescue constructs can sometimes lead to unintended rescues in other cell types due to cell-nonautonomous signaling. Because all serotonin-producing neurons also express the serotonin reuptake transporter *mod-5*, serotonin produced by one cell in our rescue strains could be taken up by other serotonin-producing neurons, leading to unintended signaling effects. This may also be true of the uv1 and RIM tyraminergic rescue strains, although little is known about tyramine reuptake in *C. elegans*. Two cells identified via tissue-specific rescue experiments (ADF and RIS, ***Figures 1G and 2D***) were also found to be necessary via cell-specific knockout (ADF *tph-1* KO, ***Figure 1E***; RIS ablation, ***Figure 2C***), decreasing the likelihood of a false positive from the rescue strain technique. However, the role of the RIM neuron was identified via a *tdc-1* rescue strain and was not validated using a RIM-specific knockout (***Figure 7B***). Therefore, the contribution of RIM signaling to this circuit is less well-validated, and a RIM-specific *tdc-1* knockout strain should be examined in future work. Finally, additional genetic controls could better support the role of RIS-specific *ser-7* expression in genetic activation of the hypoxic response. For example, a *ser-7* expressing neuron that was not a hit in our screen could also be ablated and tested for necessity in *vhl-1* mediated longevity. This experiment would test whether the ability of RIS ablation to attenuate *vhl-1*-mediated longevity is not a false positive driven by any disruption to *ser-7* expression.

Additionally, although RNAi experiments were validated using sequence confirmation and qPCR, not all RNAi hits were corroborated with genetic knockouts. This leaves open the possibility that RNAi-induced knockdown effects differ from complete genetic ablation, or that production of a given RNAi may modify bacterial metabolism in a way that indirectly modifies the hypoxic response in *C. elegans*. Finally, while the use of RNAi knockdown and genetic knockouts establishes the necessity of many signals within the *vhl-1*-mediated longevity circuit, the exact directionality of these signals remains unclear. It is possible that increased, decreased, or pulsatile changes in signaling through

these bioamines and neuropeptides are required for genetic activation of the hypoxic response to extend lifespan. Work on *C. elegans* reversal behavior has also revealed an antagonistic relationship between RIM and RIS activity facilitated by both chemical (neuropeptide and tyramine) and electrical (gap junction) signaling (**Bach et al., 2023**; **Steuer Costa et al., 2019**). This known interaction should also be interrogated in the context of how these cells may communicate following genetic induction of the hypoxic response. Future work in this area could use tools to measure or modify neuronal activity, such as calcium imaging or optogenetics, to begin answering these questions.

While many individual neurosignaling components are essential for genetic activation of the hypoxic response to extend lifespan, their epistasis is unclear (**Figure 7B**). Most components of the pathway identified in this work act downstream of *vhl-1* depletion and upstream of *fmo-2* induction (summarized in **Figure 7A and B**). However, the order of each signal between these two endpoints is only predicted based on *C. elegans* neural wiring and the overlap between various identified signals and cells. For example, we hypothesize in our working model that GABA may be produced by the RIS neuron in this circuit because RIS is the primary GABAergic neuron required for *vhl-1*-mediated longevity. Alternatively, it is possible that GABA is produced by a different cell that either acts in series or in parallel with RIS signaling. In order to determine the order of each signaling component, future studies should generate genetic manipulations to each signaling component that may mimic *vhl-1* knockout to promote longevity, cross these new strains into knockouts of other signals required for *vhl-1*mediated longevity; and measure the lifespans of each double and triple mutant. This approach would also narrow down which signals are downstream of the genetic activation of the hypoxic response and which are sufficient to extend lifespan upstream of the hypoxic response in a normoxic environment. One notable target for further exploration is the SER-7 expressing RIS neuron, which plays a role in sleep (**Steuer Costa et al., 2019**) and stress resistance (**Wu et al., 2018**), and can extend lifespan when optogenetically activated under normoxic conditions (**Busack and Bringmann, 2023**).

Another limitation of this work is that it uses lifespan as the main readout for organismal health. While genetic manipulations that extend lifespan often improve stress resistance and healthspan (**Calabrese et al., 2015**; **Zhou et al., 2011**), longevity manipulations can also have adverse effects on reproduction (**Yuan et al., 2023**; **Mautz et al., 2020**) and behavior (**Duric et al., 2016**; **Mariotti, 2015**). In this study, we find that HIF-1 stabilization in the ADF neurons does not prevent the deleterious effects of *hif-1* knockout on mobility, but that HIF-1 stabilization in the NSM neurons may attenuate age-related decline in pumping and thrashing (**Figure 1—figure supplement 1**). However, future work should examine whether other modifications to this pathway, such as manipulations to RIM, RIS, or NLP-17 signaling, influence healthspan in addition to lifespan. It will be important for future studies to determine whether various components of this pathway affect both longevity and the response to different types of stressors like oxidative stress, proteotoxic stress, and infection, as HIF-1 activity also interacts with multiple stress responses (**Bellier et al., 2009**; **Palazon et al., 2014**; **Vora et al., 2022**; **Nakazawa et al., 2016**; **Fawcett et al., 2015**).

While our understanding of this circuit is still incomplete, our findings point to several promising signaling components that could be targeted for longevity interventions. Manipulating serotonin and tyramine/adrenaline signaling pathways may offer strategies for extending lifespan, with minimal pleiotropic effects if precisely controlled. These neural targets have great potential for longevity therapeutics due to (1) the small number of neurons that can control aging-related pathways in the entire organism; (2) the availability of FDA-approved pharmaceuticals that target individual bioaminergic transporters and receptors (**Bazopoulou et al., 2017**; **Petrascheck et al., 2009**; **Huang et al., 2024**); and (3) the high conservation of neurotransmitter biology between invertebrates and mammals (**Hobert, 2013**; **Li and Kim, 2008**; **Chase and Koelle, 2007**). Further research into how these pathways can be modulated in a targeted manner could spur development of interventions that promote healthy aging and delay the onset of age-related diseases.

Methods

Strains and growth conditions

C. elegans were cultured according to established protocols (**Leiser et al., 2015**). In brief, worms were grown at 20 °C on standard solid nematode growth media (NGM). Throughout their lifespan,

the worms were fed *E. coli* OP50, except during RNA interference (RNAi) experiments, where *E. coli* HT115 was used to deliver double-stranded RNA. Transfers of worms were carried out using a platinum wire, unless stated otherwise. The RNAi strains employed are listed in ***Supplementary file 1***, while the strains used in the experiments are provided in ***Supplementary file 2***. Genotypes were verified through PCR, and RNAi imaging results were confirmed by sequencing and quantitative PCR (qPCR) before proceeding with the experiments.

Generating transgenic strains

Neuron-specific stabilized HIF-1 strains

We used the following promoters to drive cDNA of HIF-1 (P621A)::SL2::GFP in three serotonergic neuronal populations: ADF neurons (*srh-142p::* HIF-1 (P621A)), NSM neurons (*ceh-2p::* HIF-1 (P621A)), HSN neurons (*ham-2p::* HIF-1 (P621A)). All plasmids were verified via restriction digest and Sanger sequencing, and ApE files are available upon request. Plasmids were microinjected to *hif-1(ia4)* KO strain by Suny Biotech using the co-injection marker *myo-2p*::GFP and two to three transgenic lines were tested in each experiment.

Neuron-specific *tph-1* rescues

The pKA805[*srh-142p*::TPH-1] and pKA807[*ceh-2p::*TPH-1] constructs were generously provided by Dr. Kaveh Ashrafi. These constructs were injected at ~50 ng/µL with fluorescent co-injection marker *myo-2p*::mNeonGreen (15 ng/µL) or *sur-5p::sur-5::*NLSGFP (20 ng/µL) and ladder DNA (up to 100 ng/µL) into gonads of day 1 gravid adult hermaphrodites. Standard protocols were followed to isolate and obtain stable over-expression mutants (***Berkowitz et al., 2008***).

ser-7 rescue strains

Plasmid construction and microinjection was conducted by Suny Biotech to generate all *ser-7* rescue constructs. In designing the plasmids, we used the following promoters to drive cDNA of *ser-7*::SL2::GFP in different neuronal populations: full rescue (*ser-7p::ser-7)*, interneuron rescue (*glr-1p::ser-7)*, bioaminergic neuron rescue (*cat-1p::ser-7)*, glutamatergic neuron rescue (*eat-4p::ser-7*), GABAergic neuron rescue (*unc-47p::ser-7*), GABAergic motor neuron rescue (*unc-25p::ser-7*), sensory neuron rescue (*osm-6p::ser-7*), cholinergic motor neuron rescue (*acr-2p::ser-7*), cholinergic neuron rescue (*unc-17p::ser-7*), M3 and M4 neuron rescue (*ceh-28p::ser-7*), and intestinal rescue (*vha-6p::ser-7*). All plasmids were verified via restriction digest and Sanger sequencing, and ApE files are available upon request. Plasmids were microinjected by Suny Biotech using the co-injection marker *myo-2p::*GFP and two to three transgenic lines were tested in each experiment.

RIS, RIC, and BAG neuronal ablation strains

For RIS neuronal ablation strains, we purchased donor plasmid *mec-18p*::caspase-3 (p12)::nz [TU#813] (Plasmid #16082) and *mec-18p* cz::caspase-3 (p17) [TU#814] from Addgene (Plasmid #16083), and used Gibson cloning to replace *mec-18p* with *srsx-18p*. Three constructs *srsx-18p*::caspase-3(p12)::nz, *srsx-18p*::cz::caspase-3(p17), and *srsx-18p*::GFP were co-injected with fluorescent co-injection marker *myo-3p*::GFP (20 ng/µL) into the wild-type N2 strain to generate RIS genetic ablation strains. Similarly, for RIC ablation strain, *tbh-1p* was constructed into TU#813 and TU#814 to replace *mec-18p*. Three constructs *tbh-1p*::caspase-3(p12)::nz, *tbh-1p*::cz::caspase-3(p17), and *tbh-1p*::GFP were co-injected with fluorescent co-injection marker *myo-3p*::GFP (20 ng/µL) into the wild-type N2 strain to generate RIC genetic ablation strains. For BAG ablation strain, *gcy-31p* was constructed into TU#813 and TU#814 to replace *mec-18p*. Three constructs *gcy-31p*::caspase-3(p12)::nz, *gcy-31p*::cz::caspase-3(p17), and *gcy-31p*::GFP were co-injected with fluorescent co-injection marker *myo-3p*::GFP (20 ng/µL) into the wild-type N2 strain to generate BAG genetic ablation strains. All plasmids were verified via restriction digest and Sanger sequencing. ApE files available upon request. Plasmid construction and microinjection was conducted by Suny Biotech.

RIM and uv1 *tdc-1* rescue strains

Plasmid construction and microinjection was conducted by Suny Biotech to generate both *tdc-1* rescue constructs. In designing the plasmids, we used the *ocr-4* promoter to drive cDNA of *tdc-1*::SL2::GFP

in the uv1 neuroendocrine cells. To express cDNA of *tdc-1*::SL2::GFP in the RIML neuron, we used the *gcy-13* promoter. All plasmids were verified via restriction digest and Sanger sequencing, and ApE files are available upon request. Plasmids were microinjected by Suny Biotech using the co-injection marker *myo-2*p::GFP.

RNAi knockdown

For all RNAi knockdowns, worms were exposed to the RNAi treatment for two generations to achieve optimal knockdown. All RNAi clones were sourced from the Ahringer or Vidal RNAi library. Each RNAi clone was sequence-verified.

Quantitative PCR

For RNAi validation experiments, RNA was isolated from day 1 adult worms that had been grown on RNAi for two generations. For measuring *fmo-2* induction in the *hif-1(ia4);* ADF::HIF-1S strain, worms were grown on OP50, synchronized, and collected at day 1 of adulthood. RNA extraction was performed using the Direct-zol RNA Miniprep Kit (Zymo), and cDNA synthesis was carried out with the Bio-Rad iScript cDNA Synthesis Kit. Gene expression was assessed using the SYBR Green quantitative RT-PCR (***Peres et al., 2018***) system (Bio-Rad), with mRNA levels normalized to the housekeeping genes *cdc-42* and *Y45FD10.4*. Primers for RNAi validation were designed to target the 3′ UTR of each gene to avoid amplification of the bacterially produced RNAi. Gene expression was quantified using standard curves.

Lifespan measurements

Lifespan assays were conducted following previously described protocols (***Leiser et al., 2015***). Briefly, 10–15 gravid adults were transferred to NGM plates for a 3-hr timed egg lay (TEL), after which they were removed. Once the progeny reached day 1 of adulthood, 60–80 worms were placed on NGM plates containing 33 µL of 150 mM fluorodeoxyuridine (FUdR), and 100 µL of 50 mg/mL ampicillin per 100 mL of NGM. FUdR inhibits progeny development, while ampicillin prevents bacterial contamination. NGM +FUdR + Ampicillin plates were seeded with concentrated bacteria (5 x for OP50-fed lifespan assays). At least two plates per strain and condition were used for each lifespan replicate. Worms were considered dead when they failed to respond to a gentle touch with a platinum wire under a dissection microscope. Lifespan data were recorded at least three times a week until all worms were dead. To prevent escape, a barrier of 75 µL of 100 mM palmitic acid (Sigma-Aldrich) dissolved in 100% ethanol was applied along the edges of each lifespan plate. Data were analyzed using R version 4.3.1 and visualized in Adobe Illustrator 2022.

RNAi lifespans

RNAi lifespan assays were performed similarly to standard lifespan assays, with modifications to the initial timed egg lay procedure and food concentrations. To ensure maximal RNAi knockdown, worms were first TEL'ed for 3 hr on RNAi plates. The progeny from this TEL were left on RNAi plates to develop into gravid adults and then used for a second TEL under the same RNAi conditions. Progeny from the second-generation TEL were then used for the lifespan assay. RNAi bacteria (HT115) are ampicillin-resistant and can grow slowly on ampicilin-containing lifespan plates. To maintain consistent bacterial availability throughout the lifespan assay, RNAi plates were seeded with bacteria at 2 x concentration, starting from an optical density (OD_{600}) of 3.0.

Fluorescent slide microscopy

Fluorescent images for this study were captured using a Leica M165F fluorescent microscope, controlled by Leica Application Suite X (LASX) software. A minimum of 15 worms per condition were imaged at a magnification of at least ×70. For image quantification, individual worms were carefully separated to ensure they did not touch. The findWormz method (***Kitto et al., 2025***) was then used to create a pixel mask of each worm from the brightfield image and measure the fluorescent intensity of that region in the corresponding fluorescent image. A description of this method and a GitHub link to the R code is published in ***Kitto et al., 2025***. The background fluorescence was subtracted from the mean fluorescence values. Data were analyzed using R version 4.3.1 and visualized in Adobe Illustrator 2022.

Pumping assays

Pumping was measured in day 2 gravid adults, as previously described (***Leiser et al., 2015***). The number of pumps per 30 s was measured in at least 10 worms under ×100 magnification. Because food availability is known to change pumping rate, only worms on the bacterial lawn were considered in this assay. Data were plotted by R version 4.3.1 and Adobe Illustrator 2022.

Thrashing assays

Thrashing was measured in day 2 gravid adults, as previously described (***Leiser et al., 2015***). Briefly, approximately 10 worms were placed in a droplet of M9 solution. Once worms began moving at a maximum rate, their body bends were counted for 30 s. Data were plotted by R version 4.3.1 and Adobe Illustrator 2022.

30-min video recordings for velocity and movement patterns

On day 1 and day 5 of adulthood, 10–15 worms of each genotype were placed in the center of a 35 mm petri dish that was completely covered in 350 µL of OP50 bacteria (bacteria were grown overnight to an optical density OD_{600} 3.0). Worms were placed above the bright light source at the base of the microscope used for video recording for 10 min to acclimate to the light, and then 30-min video recordings were started. Videos were taken at ×3.65 magnification, and at 1 frame per second on a Leica M165F microscope using Leica Application Suite X (LASX) software and 4×4 binning. The videos were analyzed using the wrMTrck multiple object tracker plugin (wrMTrck_Batch v1.04) on FIJI (***Nussbaum-Krammer et al., 2015***; FIJI Is Just ImageJ bundled with 64-bit Java 1.8.0) to measure average speed, maximum speed, worm area, total distance traveled, and distance from the point of origin. Not all worm paths lasted the full 30-min duration of the video due to fleeing and collisions. In cases when worms fled the plate and were no longer visible during the video, the data from that worm was included if the on-plate duration was ≥10 min. In cases where worms collided and wrMTrck failed to correctly determine which worm was which after the event, the data for those worms before the collision was included if the duration was ≥10 min. In all data analysis using wrMTrck data, we confirmed that there was no significant difference in average path duration per condition. Data were plotted by R version 4.3.1 and Adobe Illustrator 2022.

Statistical analysis

The height of all bar plots represents the mean value for each condition, with error bars indicating the SEM. For comparisons involving more than two conditions, one-way ANOVA followed by post-hoc Tukey HSD tests were used to assess interactions between variables and determine statistical differences between conditions. Significance levels are indicated as *p<0.05, **p<0.01, ***p<0.001, and ****p<0.0001. For lifespan assays, statistical comparisons of survivorship curves were performed using the survfit survival analysis function in R. The log-rank test was used to compare two survival curves. To assess interactions across multiple experimental variables and for comparisons involving more than two survival curves, a Cox regression analysis was conducted using the survivalMPL package in R. For experiments with multiple biological replicates, p-values were adjusted using the Bonferroni correction. Exact sample sizes (Ns) for each experiment are provided in the source data files, and minimum sample sizes for each plot are specified in the figure legends.

Acknowledgements

National Institutes of Health grant F31AG084146-01 (ESK) National Science Foundation Graduate Research Fellowship Program DGE1841052 (ESK) National Institutes of Health grant R01AG058717.

Additional information

Competing interests

Scott F Leiser: Reviewing editor, eLife. The other authors declare that no competing interests exist.

Funding

Funder	Grant reference number	Author
National Institutes of Health	F31AG084146-01	Elizabeth S Kitto
National Science Foundation Graduate Research Fellowship Program	DGE1841052	Elizabeth S Kitto
National Institutes of Health	R01AG058717	Scott F Leiser

The funders had no role in study design, data collection and interpretation, or the decision to submit the work for publication.

Author contributions

Elizabeth S Kitto, Conceptualization, Data curation, Formal analysis, Validation, Investigation, Visualization, Methodology, Writing – original draft, Project administration, Writing – review and editing; Shijiao Huang, Conceptualization, Data curation, Formal analysis, Validation, Investigation, Visualization, Methodology, Project administration, Writing – review and editing; Mira Bhandari, Sarah A Easow, Megan L Schaller, Formal analysis, Investigation, Writing – review and editing; Cassie Tian, Emily Wang, Danielle Shave, Eugene Chung, Investigation; Rebecca L Cox, Ella Henry, Formal analysis, Investigation; Safa Beydoun, Formal analysis, Investigation, Methodology, Writing – review and editing; Hillary Miller, Conceptualization, Data curation, Formal analysis, Validation, Investigation, Methodology, Writing – review and editing; Scott F Leiser, Conceptualization, Resources, Data curation, Formal analysis, Supervision, Funding acquisition, Validation, Investigation, Visualization, Methodology, Project administration, Writing – review and editing

Author ORCIDs

Elizabeth S Kitto https://orcid.org/0000-0003-3414-1509
Shijiao Huang https://orcid.org/0000-0003-1867-4794
Scott F Leiser https://orcid.org/0000-0002-8003-2955

Peer review material

Version of Record:
Reviewer #1 (Public review): https://doi.org/10.7554/eLife.107651.3.sa1
Reviewer #2 (Public review): https://doi.org/10.7554/eLife.107651.3.sa2
Reviewer #3 (Public review): https://doi.org/10.7554/eLife.107651.3.sa3
Author response https://doi.org/10.7554/eLife.107651.3.sa4

Reviewed preprint v2
Reviewer #1 (Public review): https://doi.org/10.7554/eLife.107651.2.sa3
Reviewer #2 (Public review): https://doi.org/10.7554/eLife.107651.2.sa2
Reviewer #3 (Public review): https://doi.org/10.7554/eLife.107651.2.sa1
Author response: https://doi.org/10.7554/eLife.107651.2.sa0
eLife Assessment https://doi.org/10.7554/eLife.107651.2.sa4

Reviewed preprint v1
Reviewer #1 (Public review): https://doi.org/10.7554/eLife.107651.1.sa2
Reviewer #2 (Public review): https://doi.org/10.7554/eLife.107651.1.sa1
Reviewer #3 (Public review): https://doi.org/10.7554/eLife.107651.1.sa0
eLife Assessment https://doi.org/10.7554/eLife.107651.1.sa3

Additional files

Supplementary files

Supplementary file 1. A table of the RNAi used in this manuscript, the library source for each RNAi, and the where the RNAi was used within the manuscript.

Supplementary file 2. A table of the *C. elegans* strains used in this manuscript, the sources and genetic details of each strain, and the where the strain was used within the manuscript.

MDAR checklist

Data availability

All raw data from each figure and figure supplement is available in their respective source data. All worm strains generated in this study are available to be shared upon request from the corresponding author. All other data are included in the manuscript and/or supporting information.

References

Alkema MJ, Hunter-Ensor M, Ringstad N, Horvitz HR. 2005. Tyramine Functions independently of octopamine in the *Caenorhabditis elegans* nervous system. *Neuron* **46**:247–260. DOI: https://doi.org/10.1016/j.neuron.2005.02.024, PMID: 15848803

Bach M, Bergs A, Mulcahy B, Zhen M, Gottschalk A. 2023. Coordinated electrical and chemical signaling between two neurons orchestrates switching of motor states. *bioRxiv*. DOI: https://doi.org/10.1101/2023.01.04.522780

Banerjee N, Bhattacharya R, Gorczyca M, Collins KM, Francis MM. 2017. Local neuropeptide signaling modulates serotonergic transmission to shape the temporal organization of *C. elegans* egg-laying behavior. *PLOS Genetics* **13**:e1006697. DOI: https://doi.org/10.1371/journal.pgen.1006697, PMID: 28384151

Bauknecht P, Jékely G. 2017. Ancient coexistence of norepinephrine, tyramine, and octopamine signaling in bilaterians. *BMC Biology* **15**:6. DOI: https://doi.org/10.1186/s12915-016-0341-7, PMID: 28137258

Bazopoulou D, Chaudhury AR, Pantazis A, Chronis N. 2017. An automated compound screening for anti-aging effects on the function of *C. elegans* sensory neurons. *Scientific Reports* **7**:9403. DOI: https://doi.org/10.1038/s41598-017-09651-x, PMID: 28839194

Bellier A, Chen CS, Kao CY, Cinar HN, Aroian RV. 2009. Hypoxia and the hypoxic response pathway protect against pore-forming toxins in *C. elegans*. *PLOS Pathogens* **5**:e1000689. DOI: https://doi.org/10.1371/journal.ppat.1000689, PMID: 20011506

Berendzen KM, Durieux J, Shao L-W, Tian Y, Kim H-E, Wolff S, Liu Y, Dillin A. 2016. Neuroendocrine coordination of mitochondrial stress signaling and proteostasis. *Cell* **166**:1553–1563.. DOI: https://doi.org/10.1016/j.cell.2016.08.042, PMID: 27610575

Berkowitz LA, Knight AL, Caldwell GA, Caldwell KA. 2008. Generation of stable transgenic *C. elegans* using microinjection. *Journal of Visualized Experiments* **18**:833. DOI: https://doi.org/10.3791/833, PMID: 19066505

Bhat A, Carranza FR, Tuckowski AM, Leiser SF. 2024. Flavin-containing monooxygenase (FMO): beyond xenobiotics. *BioEssays* **46**:e2400029. DOI: https://doi.org/10.1002/bies.202400029, PMID: 38713170

Blüher M, Kahn BB, Kahn CR. 2003. Extended longevity in mice lacking the insulin receptor in adipose tissue. *Science* **299**:572–574. DOI: https://doi.org/10.1126/science.1078223, PMID: 12543978

Boylston WH, DeFord JH, Papaconstantinou J. 2006. Identification of longevity-associated genes in long-lived Snell and Ames dwarf mice. *Age* **28**:125–144. DOI: https://doi.org/10.1007/s11357-006-9008-6, PMID: 19943135

Bretscher AJ, Kodama-Namba E, Busch KE, Murphy RJ, Soltesz Z, Laurent P, de Bono M. 2011. Temperature, oxygen, and salt-sensing neurons in *C. elegans* are carbon dioxide sensors that control avoidance behavior. *Neuron* **69**:1099–1113. DOI: https://doi.org/10.1016/j.neuron.2011.02.023, PMID: 21435556

Burch JB, Augustine AD, Frieden LA, Hadley E, Howcroft TK, Johnson R, Khalsa PS, Kohanski RA, Li XL, Macchiarini F, Niederehe G, Oh YS, Pawlyk AC, Rodriguez H, Rowland JH, Shen GL, Sierra F, Wise BC. 2014. Advances in geroscience: impact on healthspan and chronic disease. *The Journals of Gerontology. Series A, Biological Sciences and Medical Sciences* **69 Suppl 1**:S1–S3. DOI: https://doi.org/10.1093/gerona/glu041, PMID: 24833579

Burtscher M. 2014. Effects of living at higher altitudes on mortality: a narrative review. *Aging and Disease* **5**:274–280. DOI: https://doi.org/10.14336/AD.2014.0500274, PMID: 25110611

Busack I, Bringmann H. 2023. A sleep-active neuron can promote survival while sleep behavior is disturbed. *PLOS Genetics* **19**:e1010665. DOI: https://doi.org/10.1371/journal.pgen.1010665, PMID: 36917595

Calabrese EJ, Dhawan G, Kapoor R, Iavicoli I, Calabrese V. 2015. What is hormesis and its relevance to healthy aging and longevity? *Biogerontology* **16**:693–707. DOI: https://doi.org/10.1007/s10522-015-9601-0, PMID: 26349923

Carre-Pierrat M, Baillie D, Johnsen R, Hyde R, Hart A, Granger L, Ségalat L. 2006. Characterization of the *Caenorhabditis elegans* G protein-coupled serotonin receptors. *Invertebrate Neuroscience* **6**:189–205. DOI: https://doi.org/10.1007/s10158-006-0033-z, PMID: 17082916

Chang AJ, Bargmann CI. 2008. Hypoxia and the HIF-1 transcriptional pathway reorganize a neuronal circuit for oxygen-dependent behavior in *Caenorhabditis elegans*. *PNAS* **105**:7321–7326. DOI: https://doi.org/10.1073/pnas.0802164105, PMID: 18477695

Chase DL, Koelle MR. 2007. Biogenic amine neurotransmitters in *C. elegans*. *WormBook* **1–15**:1–15. DOI: https://doi.org/10.1895/wormbook.1.132.1, PMID: 18050501

Conti B. 2008. Considerations on temperature, longevity and aging. *Cellular and Molecular Life Sciences* **65**:1626–1630. DOI: https://doi.org/10.1007/s00018-008-7536-1, PMID: 18425417

Davanian D, Faeghi F, ShahzadiS, Farshidfar Z. 2019. Evaluation of diffusion anisotropy and diffusion shape in grading of glial tumors. *Journal of Biomedical Physics & Engineering* **9**:459–464. DOI: https://doi.org/10.31661/jbpe.v0i0.513, PMID: 31531299

De Rosa MJ, Veuthey T, Florman J, Grant J, Blanco MG, Andersen N, Donnelly J, Rayes D, Alkema MJ. 2019. The flight response impairs cytoprotective mechanisms by activating the insulin pathway. *Nature* **573**:135–138. DOI: https://doi.org/10.1038/s41586-019-1524-5, PMID: 31462774

Duric V, Clayton S, Leong ML, Yuan L-L. 2016. Comorbidity factors and brain mechanisms linking chronic stress and systemic illness. *Neural Plasticity* **2016**:5460732. DOI: https://doi.org/10.1155/2016/5460732, PMID: 26977323

Epstein ACR, Gleadle JM, McNeill LA, Hewitson KS, O'Rourke J, Mole DR, Mukherji M, Metzen E, Wilson MI, Dhanda A, Tian YM, Masson N, Hamilton DL, Jaakkola P, Barstead R, Hodgkin J, Maxwell PH, Pugh CW, Schofield CJ, Ratcliffe PJ. 2001. *C. elegans* EGL-9 and mammalian homologs define a family of dioxygenases that regulate HIF by prolyl hydroxylation. *Cell* **107**:43–54. DOI: https://doi.org/10.1016/S0092-8674(01)00507-4, PMID: 11595184

Fawcett EM, Hoyt JM, Johnson JK, Miller DL. 2015. Hypoxia disrupts proteostasis in *Caenorhabditis elegans*. *Aging Cell* **14**:92–101. DOI: https://doi.org/10.1111/acel.12301, PMID: 25510338

Flavell SW, Pokala N, Macosko EZ, Albrecht DR, Larsch J, Bargmann CI. 2013. Serotonin and the neuropeptide PDF initiate and extend opposing behavioral states in *C. elegans*. *Cell* **154**:1023–1035. DOI: https://doi.org/10.1016/j.cell.2013.08.001, PMID: 23972393

Fontana L, Partridge L. 2015. Promoting health and longevity through diet: from model organisms to humans. *Cell* **161**:106–118. DOI: https://doi.org/10.1016/j.cell.2015.02.020, PMID: 25815989

Grady DL, Thanos PK, Corrada MM, Barnett JC Jr, Ciobanu V, Shustarovich D, Napoli A, Moyzis AG, Grandy D, Rubinstein M, Wang G-J, Kawas CH, Chen C, Dong Q, Wang E, Volkow ND, Moyzis RK. 2013. DRD4 genotype predicts longevity in mouse and human. *The Journal of Neuroscience* **33**:286–291. DOI: https://doi.org/10.1523/JNEUROSCI.3515-12.2013, PMID: 23283341

Guo J, Huang X, Dou L, Yan M, Shen T, Tang W, Li J. 2022. Aging and aging-related diseases: from molecular mechanisms to interventions and treatments. *Signal Transduction and Targeted Therapy* **7**:391. DOI: https://doi.org/10.1038/s41392-022-01251-0, PMID: 36522308

Haeussler S, Conradt B. 2022. Methods to study the mitochondrial Unfolded Protein Response (UPR^{mt}) in *Caenorhabditis elegans*. *Methods in Molecular Biology* **2378**:249–259. DOI: https://doi.org/10.1007/978-1-0716-1732-8_16, PMID: 34985705

Hallem EA, Sternberg PW. 2008. Acute carbon dioxide avoidance in *Caenorhabditis elegans*. *PNAS* **105**:8038–8043. DOI: https://doi.org/10.1073/pnas.0707469105, PMID: 18524955

Hobert O. 2013. The neuronal genome of *Caenorhabditis elegans*. *WormBook* **1–106**:1–106. DOI: https://doi.org/10.1895/wormbook.1.161.1, PMID: 24081909

Hobson RJ, Hapiak VM, Xiao H, Buehrer KL, Komuniecki PR, Komuniecki RW. 2006. SER-7, a *Caenorhabditis elegans* 5-HT7-like receptor, is essential for the 5-HT stimulation of pharyngeal pumping and egg laying. *Genetics* **172**:159–169. DOI: https://doi.org/10.1534/genetics.105.044495, PMID: 16204223

Holzenberger M, Dupont J, Ducos B, Leneuve P, Géloën A, Even PC, Cervera P, Le Bouc Y. 2003. IGF-1 receptor regulates lifespan and resistance to oxidative stress in mice. *Nature* **421**:182–187. DOI: https://doi.org/10.1038/nature01298, PMID: 12483226

Huang S, Cox RL, Tuckowski A, Beydoun S, Bhat A, Howington MB, Sarker M, Miller H, Ruwe E, Wang E, Li X, Gardea EA, DeNicola D, Peterson W, Carrier JM, Miller RA, Sutphin GL, Leiser SF. 2024. Fmo induction as a tool to screen for pro-longevity drugs. *GeroScience* **46**:4689–4706. DOI: https://doi.org/10.1007/s11357-024-01207-y, PMID: 38787463

Jacob TC, Kaplan JM. 2003. The EGL-21 carboxypeptidase E facilitates acetylcholine release at *Caenorhabditis elegans* neuromuscular junctions. *The Journal of Neuroscience* **23**:2122–2130. DOI: https://doi.org/10.1523/JNEUROSCI.23-06-02122.2003, PMID: 12657671

Kaeberlein M, Kapahi P. 2009. The hypoxic response and aging. *Cell Cycle* **8**:2324. DOI: https://doi.org/10.4161/cc.8.15.9126, PMID: 19633411

Kaeberlein M. 2013. Longevity and aging. *F1000prime Reports* **5**:5. DOI: https://doi.org/10.12703/P5-5, PMID: 23513177

Kaelin WG. 2002. Molecular basis of the VHL hereditary cancer syndrome. *Nature Reviews. Cancer* **2**:673–682. DOI: https://doi.org/10.1038/nrc885, PMID: 12209156

Kappeler L, De Magalhaes Filho C, Dupont J, Leneuve P, Cervera P, Périn L, Loudes C, Blaise A, Klein R, Epelbaum J, Le Bouc Y, Holzenberger M. 2008. Brain IGF-1 receptors control mammalian growth and lifespan through a neuroendocrine mechanism. *PLOS Biology* **6**:e254. DOI: https://doi.org/10.1371/journal.pbio.0060254, PMID: 18959478

Kirkland JL, Peterson C. 2009. Healthspan, translation, and new outcomes for animal studies of aging. *The Journals of Gerontology. Series A, Biological Sciences and Medical Sciences* **64**:209–212. DOI: https://doi.org/10.1093/gerona/gln063, PMID: 19196900

Kitto ES, Beydoun S, Leiser SF. 2024. Food touch limits lifespan through bioamine and neuroendocrine signaling. *bioRxiv*. DOI: https://doi.org/10.1101/2024.04.19.590228

Kitto E, Dean J, Leiser S. 2025. findWormz is a user-friendly automated fluorescence quantification method for *C. elegans* research. *microPublication Biology* **2025**:001562. DOI: https://doi.org/10.17912/micropub.biology.001562, PMID: 40353139

Kruempel JCP, Miller HA, Schaller ML, Fretz A, Howington M, Sarker M, Huang S, Leiser SF. 2020. Hypoxic response regulators RHY-1 and EGL-9/PHD promote longevity through a VHL-1-independent transcriptional response. *GeroScience* **42**:1621–1633. DOI: https://doi.org/10.1007/s11357-020-00194-0, PMID: 32399915
Leiser SF, Miller H, Rossner R, Fletcher M, Leonard A, Primitivo M, Rintala N, Ramos FJ, Miller DL, Kaeberlein M. 2015. Cell nonautonomous activation of flavin-containing monooxygenase promotes longevity and health span. *Science* **350**:1375–1378. DOI: https://doi.org/10.1126/science.aac9257, PMID: 26586189
Li C, Kim K. 2008. Neuropeptides. *WormBook* **1–36**:1–36. DOI: https://doi.org/10.1895/wormbook.1.142.1, PMID: 18819171
Li Y, Wang M-S, Otecko NO, Wang W, Shi P, Wu D-D, Zhang Y-P. 2017. Hypoxia potentially promotes Tibetan longevity. *Cell Research* **27**:302–305. DOI: https://doi.org/10.1038/cr.2016.105, PMID: 27608935
Libert S, Zwiener J, Chu X, Vanvoorhies W, Roman G, Pletcher SD. 2007. Regulation of *Drosophila* life span by olfaction and food-derived odors. *Science* **315**:1133–1137. DOI: https://doi.org/10.1126/science.1136610, PMID: 17272684
Lonser RR, Glenn GM, Walther M, Chew EY, Libutti SK, Linehan WM, Oldfield EH. 2003. von Hippel-Lindau disease. *Lancet* **361**:2059–2067. DOI: https://doi.org/10.1016/S0140-6736(03)13643-4, PMID: 12814730
Mariotti A. 2015. The effects of chronic stress on health: new insights into the molecular mechanisms of brain-body communication. *Future Science OA* **1**:FSO23. DOI: https://doi.org/10.4155/fso.15.21, PMID: 28031896
Mautz BS, Lind MI, Maklakov AA. 2020. Dietary restriction improves fitness of aging parents but reduces fitness of their offspring in nematodes. *The Journals of Gerontology. Series A, Biological Sciences and Medical Sciences* **75**:843–848. DOI: https://doi.org/10.1093/gerona/glz276, PMID: 31761926
Miller HA, Dean ES, Pletcher SD, Leiser SF. 2020. Cell non-autonomous regulation of health and longevity. *eLife* **9**:e62659. DOI: https://doi.org/10.7554/eLife.62659, PMID: 33300870
Miller HA, Huang S, Dean ES, Schaller ML, Tuckowski AM, Munneke AS, Beydoun S, Pletcher SD, Leiser SF. 2022. Serotonin and dopamine modulate aging in response to food odor and availability. *Nature Communications* **13**:3271. DOI: https://doi.org/10.1038/s41467-022-30869-5, PMID: 35672307
Müller R-U, Fabretti F, Zank S, Burst V, Benzing T, Schermer B. 2009. The von Hippel Lindau tumor suppressor limits longevity. *Journal of the American Society of Nephrology* **20**:2513–2517. DOI: https://doi.org/10.1681/ASN.2009050497, PMID: 19797165
Nakazawa MS, Keith B, Simon MC. 2016. Oxygen availability and metabolic adaptations. *Nature Reviews. Cancer* **16**:663–673. DOI: https://doi.org/10.1038/nrc.2016.84, PMID: 27658636
Noble T, Stieglitz J, Srinivasan S. 2013. An integrated serotonin and octopamine neuronal circuit directs the release of an endocrine signal to control *C. elegans* body fat. *Cell Metabolism* **18**:672–684. DOI: https://doi.org/10.1016/j.cmet.2013.09.007, PMID: 24120942
Nussbaum-Krammer CI, Neto MF, Brielmann RM, Pedersen JS, Morimoto RI. 2015. Investigating the spreading and toxicity of prion-like proteins using the metazoan model organism *C. elegans*. *Journal of Visualized Experiments* **52321**:52321. DOI: https://doi.org/10.3791/52321, PMID: 25591151
Ohh M, Taber CC, Ferens FG, Tarade D. 2022. Hypoxia-inducible factor underlies von Hippel-Lindau disease stigmata. *eLife* **11**:e80774. DOI: https://doi.org/10.7554/eLife.80774, PMID: 36040300
Özbey NP, Imanikia S, Krueger C. 2020. Tyramine acts downstream of neuronal XBP-1s to Coordinate Inter-tissue UPR. *Developmental Cell* **55**:754–770. DOI: https://doi.org/10.1016/j.devcel.2020.10.024, PMID: 33232669
Palamiuc L, Noble T, Witham E, Ratanpal H, Vaughan M, Srinivasan S. 2017. A tachykinin-like neuroendocrine signalling axis couples central serotonin action and nutrient sensing with peripheral lipid metabolism. *Nature Communications* **8**:14237. DOI: https://doi.org/10.1038/ncomms14237, PMID: 28128367
Palazon A, Goldrath AW, Nizet V, Johnson RS. 2014. HIF transcription factors, inflammation, and immunity. *Immunity* **41**:518–528. DOI: https://doi.org/10.1016/j.immuni.2014.09.008, PMID: 25367569
Peres TV, Arantes LP, Miah MR, Bornhorst J, Schwerdtle T, Bowman AB, Leal RB, Aschner M. 2018. Role of *Caenorhabditis elegans* AKT-1/2 and SGK-1 in manganese toxicity. *Neurotoxicity Research* **34**:584–596. DOI: https://doi.org/10.1007/s12640-018-9915-1, PMID: 29882004
Petrascheck M, Ye X, Buck LB. 2009. A high-throughput screen for chemicals that increase the lifespan of *Caenorhabditis elegans*. *Annals of the New York Academy of Sciences* **1170**:698–701. DOI: https://doi.org/10.1111/j.1749-6632.2009.04377.x, PMID: 19686215
Pirri JK, McPherson AD, Donnelly JL, Francis MM, Alkema MJ. 2009. A tyramine-gated chloride channel coordinates distinct motor programs of a *Caenorhabditis elegans* escape response. *Neuron* **62**:526–538. DOI: https://doi.org/10.1016/j.neuron.2009.04.013, PMID: 19477154
Pocock R, Hobert O. 2008. Oxygen levels affect axon guidance and neuronal migration in *Caenorhabditis elegans*. *Nature Neuroscience* **11**:894–900. DOI: https://doi.org/10.1038/nn.2152, PMID: 18587389
Powell-Coffman JA, Coffman CR. 2010. Apoptosis: Lack of oxygen aids cell survival. *Nature* **465**:554–555. DOI: https://doi.org/10.1038/465554a, PMID: 20520697
Prasad BC, Clark SG. 2006. Wnt signaling establishes anteroposterior neuronal polarity and requires retromer in *C. elegans*. *Development* **133**:1757–1766. DOI: https://doi.org/10.1242/dev.02357, PMID: 16571624
Rattan SIS. 2008. Hormesis in aging. *Ageing Research Reviews* **7**:63–78. DOI: https://doi.org/10.1016/j.arr.2007.03.002, PMID: 17964227
Rex E, Molitor SC, Hapiak V, Xiao H, Henderson M, Komuniecki R. 2004. Tyramine receptor (SER-2) isoforms are involved in the regulation of pharyngeal pumping and foraging behavior in *Caenorhabditis elegans*. *Journal of Neurochemistry* **91**:1104–1115. DOI: https://doi.org/10.1111/j.1471-4159.2004.02787.x, PMID: 15569254

Rex E, Hapiak V, Hobson R, Smith K, Xiao H, Komuniecki R. 2005. TYRA-2 (F01E11.5): a *Caenorhabditis elegans* tyramine receptor expressed in the MC and NSM pharyngeal neurons. *Journal of Neurochemistry* **94**:181–191. DOI: https://doi.org/10.1111/j.1471-4159.2005.03180.x, PMID: 15953361

Riera CE, Huising MO, Follett P, Leblanc M, Halloran J, Van Andel R, de Magalhaes Filho CD, Merkwirth C, Dillin A. 2014. TRPV1 pain receptors regulate longevity and metabolism by neuropeptide signaling. *Cell* **157**:1023–1036. DOI: https://doi.org/10.1016/j.cell.2014.03.051, PMID: 24855942

Rogers RS, Wang H, Durham TJ, Stefely JA, Owiti NA, Markhard AL, Sandler L, To TL, Mootha VK. 2023. Hypoxia extends lifespan and neurological function in a mouse model of aging. *PLOS Biology* **21**:e3002117. DOI: https://doi.org/10.1371/journal.pbio.3002117, PMID: 37220109

Shen C, Nettleton D, Jiang M, Kim SK, Powell-Coffman JA. 2005. Roles of the HIF-1 hypoxia-inducible factor during hypoxia response in *Caenorhabditis elegans*. *The Journal of Biological Chemistry* **280**:20580–20588. DOI: https://doi.org/10.1074/jbc.M501894200, PMID: 15781453

Speese S, Petrie M, Schuske K, Ailion M, Ann K, Iwasaki K, Jorgensen EM, Martin TFJ. 2007. UNC-31 (CAPS) is required for dense-core vesicle but not synaptic vesicle exocytosis in *Caenorhabditis elegans*. *Journal of Neuroscience* **27**:6150–6162. DOI: https://doi.org/10.1523/JNEUROSCI.1466-07.2007, PMID: 17553987

Steuer Costa W, Van der Auwera P, Glock C, Liewald JF, Bach M, Schüler C, Wabnig S, Oranth A, Masurat F, Bringmann H, Schoofs L, Stelzer EHK, Fischer SC, Gottschalk A. 2019. A GABAergic and peptidergic sleep neuron as a locomotion stop neuron with compartmentalized Ca2+ dynamics. *Nature Communications* **10**:4095. DOI: https://doi.org/10.1038/s41467-019-12098-5, PMID: 31506439

Stewart TM, Bhapkar M, Das S, Galan K, Martin CK, McAdams L, Pieper C, Redman L, Roberts S, Stein RI, Rochon J, Williamson DA, CALERIE Study Group. 2013. Comprehensive assessment of long-term effects of reducing intake of energy phase 2 (CALERIE Phase 2) screening and recruitment: methods and results. *Contemporary Clinical Trials* **34**:10–20. DOI: https://doi.org/10.1016/j.cct.2012.08.011, PMID: 22981898

Sze JY, Victor M, Loer C, Shi Y, Ruvkun G. 2000. Food and metabolic signalling defects in a *Caenorhabditis elegans* serotonin-synthesis mutant. *Nature* **403**:560–564. DOI: https://doi.org/10.1038/35000609, PMID: 10676966

Taylor SR, Santpere G, Weinreb A, Barrett A, Reilly MB, Xu C, Varol E, Oikonomou P, Glenwinkel L, McWhirter R, Poff A, Basavaraju M, Rafi I, Yemini E, Cook SJ, Abrams A, Vidal B, Cros C, Tavazoie S, Sestan N, et al. 2021. Molecular topography of an entire nervous system. *Cell* **184**:4329–4347. DOI: https://doi.org/10.1016/j.cell.2021.06.023, PMID: 34237253

Thacker C, Rose MA. 2000. A look at the *Caenorhabditis elegans* Kex2/Subtilisin-like proprotein convertase family. *BioEssays: News and Reviews in Molecular, Cellular and Developmental Biology* **22**:545–553. DOI: https://doi.org/10.1002/(SICI)1521-1878(200006)22:6<545::AID-BIES7>3.0.CO;2-F

Turek M, Besseling J, Spies JP, König S, Bringmann H. 2016. Sleep-active neuron specification and sleep induction require FLP-11 neuropeptides to systemically induce sleep. *eLife* **5**:e12499. DOI: https://doi.org/10.7554/eLife.12499, PMID: 26949257

Veuthey T, Florman JT, Giunti S, Romussi S, De Rosa MJ, Alkema MJ, Rayes D. 2024. The neurohormone tyramine stimulates the secretion of an insulin-like peptide from the *Caenorhabditis elegans* intestine to modulate the systemic stress response. *PLOS Biology* **23**:e3002997. DOI: https://doi.org/10.1371/journal.pbio.3002997, PMID: 39874242

Vora M, Pyonteck SM, Popovitchenko T, Matlack TL, Prashar A, Kane NS, Favate J, Shah P, Rongo C. 2022. The hypoxia response pathway promotes PEP carboxykinase and gluconeogenesis in *C. elegans*. *Nature Communications* **13**:6168. DOI: https://doi.org/10.1038/s41467-022-33849-x, PMID: 36257965

Wind JJ, Lonser RR. 2011. Management of von Hippel-Lindau disease-associated CNS lesions. *Expert Review of Neurotherapeutics* **11**:1433–1441. DOI: https://doi.org/10.1586/ern.11.124, PMID: 21955200

Wolkow CA, Kimura KD, Lee MS, Ruvkun G. 2000. Regulation of *C. elegans* life-span by insulinlike signaling in the nervous system. *Science* **290**:147–150. DOI: https://doi.org/10.1126/science.290.5489.147, PMID: 11021802

Wragg RT, Hapiak V, Miller SB, Harris GP, Gray J, Komuniecki PR, Komuniecki RW. 2007. Tyramine and octopamine independently inhibit serotonin-stimulated aversive behaviors in *Caenorhabditis elegans* through two novel amine receptors. *The Journal of Neuroscience* **27**:13402–13412. DOI: https://doi.org/10.1523/JNEUROSCI.3495-07.2007, PMID: 18057198

Wu Y, Masurat F, Preis J, Bringmann H. 2018. Sleep counteracts aging phenotypes to survive starvation-induced developmental arrest in *C. elegans*. *Current Biology* **28**:3610–3624.. DOI: https://doi.org/10.1016/j.cub.2018.10.009, PMID: 30416057

Yuan R, Hascup E, Hascup K, Bartke A. 2023. Relationships among development, growth, body size, reproduction, aging, and longevity - trade-offs and pace-of-Life. *Biochemistry. Biokhimiia* **88**:1692–1703. DOI: https://doi.org/10.1134/S0006297923110020, PMID: 38105191

Zhang Y, Shao Z, Zhai Z, Shen C, Powell-Coffman JA. 2009. The HIF-1 hypoxia-inducible factor modulates lifespan in *C. elegans*. *PLOS ONE* **4**:e6348. DOI: https://doi.org/10.1371/journal.pone.0006348, PMID: 19633713

Zhang G, Li J, Purkayastha S, Tang Y, Zhang H, Yin Y, Li B, Liu G, Cai D. 2013. Hypothalamic programming of systemic ageing involving IKK-β, NF-κB and GnRH. *Nature* **497**:211–216. DOI: https://doi.org/10.1038/nature12143, PMID: 23636330

Zhou KI, Pincus Z, Slack FJ. 2011. Longevity and stress in *Caenorhabditis elegans*. *Aging* **3**:733–753. DOI: https://doi.org/10.18632/aging.100367, PMID: 21937765

Zimmer M, Gray JM, Pokala N, Chang AJ, Karow DS, Marletta M, Hudson ML, Morton DB, Chronis N, Bargmann CI. 2009. Neurons detect increases and decreases in oxygen levels using distinct guanylate cyclases. *Neuron* **61**:865–879. DOI: https://doi.org/10.1016/j.neuron.2009.02.013, PMID: 19323996

Appendix 1

Appendix 1—key resources table

Reagent type (species) or resource	Designation	Source or reference	Identifiers	Additional information
Gene (*C. elegans*)	*vhl-1*	GenBank/ Wormbase	WormBase:WBGene00006922	
Gene (*C. elegans*)	*hif-1*	GenBank/ Wormbase	WormBase:WBGene00001851	
Gene (*C. elegans*)	*fmo-2*	GenBank/ Wormbase	WormBase:WBGene00001477	
Strain, strain backgrounds (*C. elegans*)	>10 strains, please see ***Supplementary file 2***	>10 strains, please see ***Supplementary file 2***	>10 strains, please see ***Supplementary file 2***	All strains backcrossed to lab-specific N2 WT strain and validated through sequencing and/or PCR genotyping.
Transfected constructs (*E. coli*)	>10 *E. coli* strains expressing RNAi against *C. elegans* genes, please see ***Supplementary file 1***.	From Vidal and Ahringer RNAi libraries	>10 *E. coli* strains expressing RNAi against *C. elegans* genes, please see ***Supplementary file 1***.	All constructs sequence-validated.
Sequence-based reagent	Stabilized HIF-1 (HIF-1S)	Original sequence from ***Leiser et al., 2015***. Expressed in NSM and ADF neurons in this paper.	Transgene sequence, introns and exons, introns and exons	ATGGAAGACAATCGGAAAAGgtagagttagaattctgttagaatcgaaattcattcttaaacattccatgattggatgcctgaaaa cgctagaagtaccgtagtcctttgggtttgctccatgctctgctcgcaaatgagagagagggagcattggcagaggtagatgtattgaaaatgc gcatttccgaatcgaatatcaaatgtgaatcatctatataaaatatatctcgctctttttagacacaactcatttttaatcggagatgttagataaagt aaattatgaaaataaattgtgaaataattgtgattgaaggtggagtagcgccagtggcagttttgcctaaaaaatacacttacaatggctcgaa acaaccaaaaatcataataaaacacttaaaaatttttagattttcataatttccggtcaaagttttggcaaatggccaaaatttttacaaacata agtatttgaggaatgccgcatgttccgatccctactatgcttccaaaattatgagtggcaaaaattgagtgattatcatctaacggacggtaaa taaacaatttcaaaaaatttttgacaatttttaatttgatattcggtcattttagtaccattggattagttttcaacactttctccactggctcctcctact ccacctttgaaaaaataaatttttcccagtttatacttaaaactaaattaaatcgaaaaacctcatgagaagtgtacttatataggtatataatttttt gaaattcaccaatttttggggtgacaagaaattcaaaatcaaacttttttagAAACATGGAACGCCGTCGTGAAACATCGAG ACACGCGGCTCGTGATCGTCGGTCTAAAGAATCGGATATATTTGATGATCTGAAAATGTGTGTGC CTATTGTTGAAGAAGGTACCGTAACTCATCTAGACCGTATTGCACTTCTTCGTGTTGCCGCCACA ATTTGTCGACTGCGCAAGACAGCCGGTAATGgtaagtgacatcgaataaagaaatagttgattcaacatcaaaaatca cttgaaaatcgtgttttatgctgagaaaatcgaccaaaaatcactgccaatttttctcaaattaatatttttctttcagTATTGGAAAACAATT TGGACAATGAAATCACAAATGAGGTATGGACTGAAGACACCATCGCCGAATGCTTGGACGGCTTT GTTATGATTGTTGACAGTGATTCTTCAATTCTTTACGTCACTGAAAGTGTTGCAATGTATTTAGGATT AACACAGgtgagcaatagaaaacttgcttctttaacatcgatatattttcagACAGATTTAACAGGTCGAGCCCTTCGAGA CTTTCTTCATCCATCCGACTATGACGAGTTTGACAAGCAATCAAAAATGCTGCACAAGCCACGTGG CGAGGACACAGACACCACCGGCATCAACATGGTGCTTCGAATGAAGACAGTCATCAGCCCACGT GGAAGATGTCTGAATTTGAAGAGTGCTTTGTACAAATCAGTGTCTTTCCTGGTTCATTCAAAAGTTT CAACTGGTGGACACGTGTCATTCATGCAAGGTATCACAATTCCTGCTGGACAGGGTACAACTAATG CAAATGCATCTGCAATGACAAAGgtgaatatctgctttgaatgtttcatagtaagattctaaagtttgaacttttgatcttgggaatttct gctcctcctttccgcttcttgataaactgatggaattgtgagacaaaatgttgagtagacgttacacaatttcattttcttcttattcttctgctcgctcg aaaagtttgttcttttgatctttaaaatagagaatagtgctttgagcaaagcacactcagccgttggcacctcgcgcatagaaaacaggattaga aaattggagagaagtagagaagcacaagcacatgcaacttggcgtcatcttctccttttttgaagcagaagagaaaacggagaagatgtt acatcttgtattgctgctccgtttgcaaaagtaaaatgagcagggactctgaatacctagatagaaaagtgagtcctaaagggcgtgtatatt cgaaaactttttcaaatcagatttatagatgctataagtttaataaaaatatagatggattaatttacagTACACGGAAAGCCCAAT GGGTGCATTCACAACTCGTCACACTTGCGACATGCGCATCACTTTCGTTTCGGATAAGTTCAAT TACATCTTGAAAAGTGAGCTGAAGACTCTCATGGGCACCAGTTTCTACGAATTGGTACATCCAG CCGATATGATGATAGTATCAAAATCCATGAAGGAACTTTTTGCCAAAGGACACATCCGTACCCCG TATTACCGGTTGATTGCTGCAAATGACACACTTGCCTGGATTCAAACAGAAGCTACTACAATCA CACATACGACGAAAGGACAAAAAGGACAATATGTCATTTGTGTTCATTACGTTCTCGGAATCCA AGGAGCTGAAGAGTCATTGGTAGTTTGCACTGATTCAATGCCAGCTGGAATGCAAGTAGATATC AAGAAGGAAGTGGATGATACAAGAGACTATATTGGAAGACAACCTGAAATTGTGGAATGCGTC GATTTTACTCCATTGATCGAGCCAGAAGATCCATTTGATACGGTTATTGAGCCAGTCGTTGGTG GAGAAGAACCTGTTAAGCAGGCTGATATGGgtaagtacatgtttaagaacgtattaaaagtttgtaattatacagtttga ttcacctaagttttttttatccaaattgaataatttacgaggtacgtatataggaatttattcggtgacggatgagtatgagcaacgtgtttatgg gcaaatttctgccggcaatgatatagaagactgcgatatggattctgatacagaatccatagaagattccggttagcaccggaattcga tgtggatctggctccgatttataatgagaaaatggaagttgacggagaggatgaggacggcggagaggaggtactttgggaaatggg attatgattactaagttaaaaaaacaacgatcgcagttttcccctccgttgtcctcatacctccgtgagtttctcttttttcttatttttcaaacttgt caaacttgtccatgcatgtcgtattatttttttaccctacgcctactcaaagttccatacatttagcaagtgatttcttaacgtgtgtatttcagGA GCACGTAAGAACAGCTACGATGACGTTTTGCAATGGCTTTTTCGCGACCAGCCAAGCTCTC CGCCGCCGGCACGCTACCGGTCAGCGGACCGCTTCAGGACAACCGAACCGTCGAATTTCG GTTCCGCTCTGGCCTCGCCGGACTTCATGGATTCGTCATCTCGTACCTCCCGACCGAAGAC ATCATACGGACGAAGAGCACAAAGTCAGGGAAGTCGAACAACTGGATCGTCTTCCACGTCA GCATCGGCCACATTGCCACACAGTGCCAACTACTCGCCACTTGCAGAGGGCATCTCACAAT GTGGACTTAACAGTCCCCCGAGgttagttttttatacatttttcacaattagcacgttgagcatgtacatgtttataatatccttg tatcagttgcagTATCAAATCTGGACAAGTCGTGTACGGAGACGCTCGATCTATGGGACGTAGCTG CGATCCGTCCGATTCGTCACGACGCTTTTCCGCCCTTTCACCATCAGATACTCTCAATGTGTC GTCCACTAGAGGCATCAACCCAGTCATCGGAAGCAATGATGTGTTCTCCACTATGCCTTTTGC CGATTCTATCGCCATTGCCGAAAGGATCGATTCGTCGCCAACATTAACCTCTGGCGAACCAAT ACTTTGTGgttagttttttttaaatgttcaaatcaatctcattcgtgaaagaaatcagataactttcaacaaaatgtttaactttcagACG ATCTTCAATGGGAAGAGCCTGATTTATCGTGCTTGGCAGCATTCGTTGACACTTATGATATGAT GCAAATGGACGAGGGGTTACCACCAGAGCTTCAAGCTCTTTACGACTTGCCTGACTTTACAC CTGCGGTACCTCAAGCCCCAGCTGCTCGGCCTGTGCACATTGACgtaagcctgttttgtttttggctcctaa cattatgttaatttttgcagAGAAGCCCACCAGCGAAGCGAATGCACCAATCAGGTCCCTCAGATTTAGA TTTTATGTACACTCAACATTATCAACCATTCCAACAAGACGAGACATATTGGCAAGGACAGCAA CAGCAAAATGAACAACAGCCTAGTTCTTATTCCCCATTTCCAATGCTCTCTTGA

Appendix 1 Continued on next page

Appendix 1 Continued

Reagent type (species) or resource	Designation	Source or reference	Identifiers	Additional information
Sequence-based reagent	nlp-17_F	This paper	qPCR primers	CTCTTCTGCCTTTTGGTTTTGGT
Sequence-based reagent	Nlp-17_R	This paper	qPCR primers	TGGGGGACGCATTACATCCTG
Sequence-based reagent	hsp-6_F	This paper	qPCR primers	CAAACTCCTGTGTCAGTATCATGGAAGG
Sequence-based reagent	hsp-6_R	This paper	qPCR primers	GCTGGCTTTGACAATCTTGTATGGAACG
Sequence-based reagent	Fmo-2_F	This paper	qPCR primers	GGAGCTGGTGCTTCTGGATT
Sequence-based reagent	Fmo-2_R	This paper	qPCR primers	TTCGAGGTGTTGATCACGGT
Sequence-based reagent	Tyra3F	This paper	qPCR primers	TCCTTCGGATGCGTTCAACA
Sequence-based reagent	Tyra3R	This paper	qPCR primers	ACGGGAGAGGGGAAATCAAC
Sequence-based reagent	Vhl1F	This paper	qPCR primers	TTGCCGGACGTTCGTTCTTA
Sequence-based reagent	Vhl1R	This paper	qPCR primers	AACGACCGTATGGGGAATGG
Sequence-based reagent	Ser-2_F	This paper	qPCR primers	ACACTGATTCGGTGCAGGAAA
Sequence-based reagent	Ser-2_R	This paper	qPCR primers	AACCAGCTCGACAGTTGGAA
Sequence-based reagent	Tyra-2_F	This paper	qPCR primers	TCCCCACTGTCACACAACAA
Sequence-based reagent	Tyra-2_R	This paper	qPCR primers	GCTCATCACATAACTCGACATCA
Sequence-based reagent	Lgc-55_F	This paper	qPCR primers	GGAGAAGGCAGCCACAAGAA
Sequence-based reagent	Lgc-55_R	This paper	qPCR primers	GGCACCCTCTTCATGCTCA